

Mechanism for modulation of gating of connexin26-containing channels by taurine

Darren Locke,¹ Fabien Kieken,² Liang Tao,³ Paul L. Sorgen,² and Andrew L. Harris¹

¹Department of Pharmacology and Physiology, New Jersey Medical School, University of Medicine and Dentistry of New Jersey, Newark, NJ 07103

²Department of Biochemistry and Molecular Biology, University of Nebraska Medical Center, Omaha, NE 68198

³Department of Pharmacology, Zhongshan School of Medicine, Sun Yat-Sen University, Guangzhou, Guangdong Province 510089, China

The mechanisms of action of endogenous modulatory ligands of connexin channels are largely unknown. Previous work showed that protonated aminosulfonates (AS), notably taurine, directly and reversibly inhibit homomeric and heteromeric channels that contain Cx26, a widely distributed connexin, but not homomeric Cx32 channels. The present study investigated the molecular mechanisms of connexin channel modulation by taurine, using hemichannels and junctional channels composed of Cx26 (homomeric) and Cx26/Cx32 (heteromeric). The addition of a 28-amino acid “tag” to the carboxyl-terminal domain (CT) of Cx26 (Cx26_T) eliminated taurine sensitivity of homomeric and heteromeric hemichannels in cells and liposomes. Cleavage of all but four residues of the tag (Cx26_{Tc}) resulted in taurine-induced pore narrowing in homomeric hemichannels, and restored taurine inhibition of heteromeric hemichannels (Cx26_{Tc}/Cx32). Taurine actions on junctional channels were fully consistent with those on hemichannels. Taurine-induced inhibition of Cx26/Cx32_T and nontagged Cx26 junctional channels was blocked by extracellular HEPES, a blocker of the taurine transporter, confirming that the taurine-sensitive site of Cx26 is cytoplasmic. Nuclear magnetic resonance of peptides corresponding to Cx26 cytoplasmic domains showed that taurine binds to the cytoplasmic loop (CL) and not the CT, and that the CT and CL directly interact. ELISA showed that taurine disrupts a pH-dependent interaction between the CT and the CT-proximal half of the CL. These studies reveal that AS disrupt a pH-driven cytoplasmic interdomain interaction in Cx26-containing channels, causing closure, and that the Cx26CT has a modulatory role in Cx26 function.

INTRODUCTION

There is scant information about the regulation of connexin channels by cytoplasmic ligands, despite the importance of gap junction channels in development, physiology, and disease. Identification of ligands and determination of their modes of action on connexin channels would be of considerable value for understanding intercellular signaling pathways and for studies of connexin channel structure–function (Harris, 2001; Hervé and Sarrouilhe, 2005).

Connexin proteins compose gap junction channels. Because they are permeable to small cytoplasmic molecules, gap junction channels mediate a direct and intimate form of intercellular molecular signaling. Junctional channels are composed of two hexameric subunits, called “hemichannels” or “connexons,” which dock end-to-end. These may be homo-oligomers or hetero-oligomers of connexins. Hemichannels are functional single-membrane channels implicated in a variety of

cellular processes distinct from those mediated by gap junction channels (Goodenough and Paul, 2003).

Many compounds affect gap junctions when applied to cells. However, in most cases it is unclear or unlikely there is direct interaction with the connexin channels (Harris, 2001; Hervé and Sarrouilhe, 2005; Spray et al., 2006). Regulation of some connexin channels by pH has been well studied (Hirst-Jensen et al., 2007); calmodulin regulates some connexin channels, but the molecular mechanism of its regulation is unknown (Lurtz and Louis, 2007).

Previous work using connexin hemichannels, purified from rodent tissues and reconstituted into liposomes, showed that the protonated forms of Good’s pH buffers (e.g., HEPES, MES, TAPS; Good et al., 1966) directly and reversibly inhibited hemichannels that contained connexin26 (Cx26), whether alone (homomeric) or with Cx32 (heteromeric) (Bevans and Harris, 1999; Locke et al., 2004b; Tao and Harris, 2004). The effect of the protonated form of these buffers accounted for the apparent

Correspondence to Darren Locke: lockedad@gmail.com

Abbreviations used in this paper: AFM, atomic force microscopy; AS, aminosulfonate(s); CL, cytoplasmic loop; CT, carboxyl-terminal domain; LPPG, 1-palmitoyl-2-hydroxy-*sn*-glycero-3-[phospho-RAC-(1-glycerol)]; NMR, nuclear magnetic resonance; PTM, posttranslational modification; TSF, transport-specific fractionation.

© 2011 Locke et al. This article is distributed under the terms of an Attribution–Noncommercial–Share Alike–No Mirror Sites license for the first six months after the publication date (see <http://www.rupress.org/terms>). After six months it is available under a Creative Commons License (Attribution–Noncommercial–Share Alike 3.0 Unported license, as described at <http://creativecommons.org/licenses/by-nc-sa/3.0/>).

pH sensitivity of the liposome-reconstituted channels. This inhibition did not occur for hemichannels composed solely of Cx32. Because Good's pH buffers are aminosulfonates (AS), the ubiquitous biological AS taurine (β -aminosulfonic acid) was tested and found to be inhibitory at cytoplasmic concentrations. Similar effects were seen for other cytoplasmic AS (e.g., hypotaurine, L-cysteic acid, L-homocysteic acid, L-cysteine sulfinic acid). Several related cytoplasmic compounds antagonized this inhibition (e.g., β -alanine, glycine, GABA, L-glutamic acid), suggesting that control of intercellular communication involves complex interplay among these compounds. The chemical requirements for the inhibition are well characterized; the protonated amine of AS is required for binding connexin, whereas the sulfonate moiety, and its proper distance relation to the amine, is necessary for the functional effect (Tao and Harris, 2004).

The AS effect was structurally corroborated by atomic force microscopy (AFM) of isolated hemichannels, revealing pore closure of Cx26 channels only in the presence of protonated AS (Yu et al., 2007). The intercellular location of gap junction channels presents challenges for detailed biological and biophysical investigation; hemichannels have proved more amenable for study *ex vivo* and, by and large, the properties of junctional channels are predictable from those of the component hemichannels (Harris, 2001; Beahm and Hall, 2002; Contreras et al., 2003; Bukauskas and Verselis, 2004; Srinivas et al., 2005).

Using taurine, which is essentially fully protonated at physiological pH (pK_a 8.8 at 37°C), the present study was undertaken to further define the molecular basis of AS inhibition of Cx26-containing channels, which are found in many tissues, including brain, skin, cochlea, liver, uterus, and liver, and whose dysfunction has a multitude of pathological consequences (Zhang and Nicholson, 1989; Willecke et al., 2002; Lee and White, 2009; Zoidl and Dermietzel, 2010). This was addressed using hemichannels and gap junction channels formed by heterologously expressed Cx26 or Cx32, and combinations, with and without an epitope tag on the carboxyl-terminal domain (CT) (Koreen et al., 2004). This tag facilitated hemichannel purification for study in liposomes and was cleavable by thrombin from purified hemichannels leaving a short (four-amino acid) addition to the CT. Hemichannel activity was also assessed in cultured cells by exploiting the ability of unpaired plasma membrane hemichannels to open when at low extracellular calcium concentrations and take up extracellular dye(s) (Li et al., 1996; Quist et al., 2000). Hemichannel results from liposome and cell studies were corroborated by studies of intercellular dye permeability through junctional channels using a donor-recipient dye transfer assay (Goldberg et al., 1995). The specific molecular interactions and their determinants were

investigated by nuclear magnetic resonance (NMR) and ELISA.

The results show that the properties of AS-induced closure previously seen using hemichannels reconstituted into liposomes are also observed for hemichannels and junctional channels in native membranes, the latter having the same AS sensitivity as their component hemichannels. The results identify the CT of Cx26 as a key component of the channel modulation, suggesting a mechanism by which AS disrupts a pH-dependent association between the CT and cytoplasmic loop (CL) of Cx26, leading to occlusion of the pore.

MATERIALS AND METHODS

Reagents

Components of the "Tet-On" connexin expression system (Koreen et al., 2004) were from BD. HEPES-buffered DMEM and bicarbonate-buffered DMEM (for experimental and maintenance media, respectively), penicillin, streptomycin, puromycin, G418 sulfate, hygromycin, and doxycycline (dox) were from Life Technologies. Agarose-conjugated anti-hemagglutinin (anti-HA) clone HA-7 mouse IgG was from Sigma-Aldrich, as were other reagents unless stated otherwise. The following lipids were from Avanti Polar Lipids, Inc.: egg phosphatidylcholine (PC), bovine brain phosphatidylserine (PS), lissamine rhodamine B-labeled egg phosphatidylethanolamine (rhod-PE), and 1-palmitoyl-2-hydroxy-*sn*-glycero-3-[phospho-RAC-(1-glycerol)] (LPPG). Detergent, *n*-octyl β D-glucoside (OG; 99.5% purity), was from Glycon Biochemicals. Bio-Gel gel filtration matrix (A; 0.5 m; 100–200 mesh; exclusion limit, 500 kD) was from Bio-Rad Laboratories. Dyes, including CM-DiI, calcein-AM, and calcein were from Invitrogen. Peptides were purchased from AnaSpec, synthesized by the University of Medicine and Dentistry of New Jersey Molecular Research Core, or purified from bacteria, as outlined below.

HeLa cells stably expressing Cx26

A HeLa clonal cell line that stably expresses nontagged Cx26 was provided by G. Sosinsky (University of California, San Diego, San Diego, CA) (Hand et al., 2002; Yu et al., 2007). These cells were maintained in DMEM containing 10% vol/vol FBS, 100 U/ml penicillin, 100 μ g/ml streptomycin, 2 mM glutamine, and 1 mg/ml puromycin.

Expression of tagged connexin channels in HeLa cells

Bidirectional tetracycline-responsive expression vectors (Takara Bio Inc.) were used to regulate expression of homomeric or heteromeric connexin hemichannels in HeLa cells. For homomeric hemichannels, rat connexin coding sequences were subcloned in-frame with a sequence coding for a 28-amino acid CT tag consisting of a thrombin cleavage site followed by a hemagglutinin epitope (HA, not His-Ala) and six repeats of His-Asn (i.e., HA(HN)₆ tag). When the two cloning sites contained different connexin coding sequences, only one connexin was tagged. Tet-On cell lines were maintained in 200 μ g/ml hygromycin and 100 μ g/ml G418. Channels are designated as Cx26_T or Cx32_T when homomeric and Cx26_T/Cx32 or Cx26/Cx32_T when heteromeric.

Purification of tagged connexin channels

Tet-On HeLa cells, 35% confluence at 2,000/cm², were induced for connexin expression with 1 μ g/ml dox. After 48 h, cells were solubilized in 50 mM NaH₂PO₄, 50 mM NaCl, 5 mM EDTA, 5 mM EGTA, 80 mM OG, 1 mM β -mercaptoethanol, 0.5 mM diisopropyl

fluorophosphate (EMD), and 0.75 mg/ml azolectin, pH 7.5, for 2 h at 4°C with rocking. Solubilization of gap junctions with OG yields intact hemichannels (Lampe et al., 1991; Harris et al., 1992; Rhee et al., 1996; Bevens et al., 1998).

The supernatant (100,000 g_{av} [g value averaged over length of centrifuge tube; e.g., at the midpoint of the tube] for 30 min at 4°C) was incubated with 0.25 ml of agarose-immobilized anti-HA mouse IgG overnight at 4°C with shaking. The antibody matrix was collected at 700 g_{av} (1 min at 4°C) and washed in a fritted column with 20 ml of 10 mM PBS, 1 M NaCl, 80 mM OG, and 1 mg/ml azolectin, pH 7.4, followed by 20 ml of the same solution containing 138 mM NaCl. Hemichannels were eluted with 50 mM CH₃COOH·Na, 0.5 M NaCl, 10 mM KCl, 1 mM EDTA, and 80 mM OG, pH 4.0, and ~0.6-ml fractions collected into ~0.05 ml of 1 M NaHCO₃, 10 mM KCl, and 80 mM OG, pH 9.0. The final pH was ~7.4.

Tag cleavage

200 μ l of purified protein was incubated with 2 U of restriction-grade thrombin (EMD) for 18 h at 4°C. Tag cleavage leaves four amino acids on the CT (LVPR), part of the thrombin cleavage site. Hemichannels with cleaved tags are designated as Cx26_{Tc} or Cx32_{Tc} when homomeric and Cx26_{Tc}/Cx32 or Cx26/Cx32_{Tc} when heteromeric.

Channel reconstitution

Immunopurified connexin hemichannels (in urea buffer, see below; 80 mM OG and 10 mg/ml PC/PS/rhod-PE at molar ratio 2:1:0.01; 200 μ l) were reconstituted into unilamellar liposomes by gel filtration in chilled, degassed urea buffer (10 mM Tris, pH 7.6, 10 mM KCl, 0.1 mM EDTA, and 459 mM urea). Two methods were used, giving identical results: an ~24-ml bed of 0.5 m Bio-Gel A (100–200 mesh media; exclusion 500 kD) (Locke et al., 2004a) or centrifugation (700 g_{av} for 1 min at 4°C) through a 1-ml column of Sephadex G-50 (Heginbotham et al., 1998). The protein/lipid ratio corresponded to an amount of connexin equivalent to less than one hemichannel per liposome so that, by design, some liposomes did not contain hemichannels.

Transport-specific fractionation (TSF) assay

TSF was used to assess the molecular selectivity of reconstituted connexin hemichannels (Harris et al., 1992; Rhee et al., 1996; Bevens et al., 1998; Bevens and Harris, 1999; Harris, 2001; Locke et al., 2004a,b, 2005; Tao and Harris, 2004, 2007; Ayad et al., 2006). TSF fractionates liposomes containing connexin hemichannels into two discrete populations within an iso-osmolar density gradient, based on hemichannel permeability to urea and sucrose, uncharged solutes that permeate open connexin hemichannels and have different density at iso-osmolar concentrations (urea buffer, density [ρ] = 1.0055 g/ml; when 400 mM sucrose replaces urea, ρ = 1.0511 g/ml; both 500 mOsm/kg). Liposomes are formed in, and entrap, urea buffer and are then centrifuged through linear iso-osmotic TSF density gradients formed from urea and sucrose buffers (300,000 g_{av} for 3 h at 37°C; slow acceleration, no brake). Equilibration of these solutes across the liposome through an open hemichannel occurs rapidly and increases the density of the liposome. TSF therefore reports all-or-nothing permeation of urea and sucrose through connexin hemichannels on a per-liposome basis. Fractionation of liposomes into bands is monitored by the fluorescence of rhod-PE (λ_{ex} = 570 nm and λ_{em} = 590 nm) in the liposome membrane. The typical positions of the upper and lower bands are centered at densities of approximately ρ = 1.02 g/ml and ρ = 1.04 g/ml, respectively. Liposomes that contain hemichannels permeable to one solute but not the other undergo osmotically driven shrinkage that results in a band of intermediate density of approximately ρ = 1.03 g/ml. Because the addition of AS to the TSF gradients could affect the densities

of the solutions, the bands were assigned as upper, intermediate, and lower on the basis of density, as determined by refractometry at 25°C (Locke et al., 2004a). Channel activity is assessed as the fraction of the liposomes that are at the lower density.

Aminosulfonate effect

The effect of AS on reconstituted hemichannel activity was assessed by exposure to AS during the TSF centrifugation. Any significant hemichannel permeability results in sufficient solute exchange to move liposomes to the lowest banding position. Therefore, TSF is an all-or-none assay of per-liposome hemichannel permeability and reports only conditions resulting in complete or near complete pore closure. Stated another way, only complete block of solute permeability by AS through the connexin hemichannel will cause a liposome containing a functional hemichannel to remain at the upper position in TSF gradients. Such a change can be a result of pore block or of reduction to near zero channel open probability. Inhibition of activity because of AS is therefore assessed as the decrease in the fraction of liposomes in the lower band compared with the corresponding control.

Correction for more than one channel per liposome

A Poisson distribution describes the maximum/minimum fraction of liposomes that will have functional hemichannels at different ratios (λ) of channels to liposomes (Rhee et al., 1996). λ is estimated from the maximum activity observed (percentage, p , of liposomes with n active hemichannels; Eq. 1):

$$p(n) = e(-\lambda) \cdot \frac{\lambda^n}{n!} \cdot 100. \quad (1)$$

As λ increases, the fraction of liposomes with two or more hemichannels increases. Therefore, the number of liposomes in the TSF lower band may not accurately reflect AS sensitivity per hemichannel (e.g., if there are two hemichannels, both would have to be inhibited for a liposome to remain at the upper position, thereby resulting in less apparent activity of a modulator). Using the Poisson distribution, λ was used to calculate the distribution of n hemichannels in the liposome population, which was used to compensate for the error introduced by some liposomes containing more than one hemichannel. This calculation transforms the fraction of liposomes in the lower TSF band to the fraction of hemichannels that are not inhibited.

Normalization of TSF data

For each preparation of connexin, for each experiment, the fraction of liposomes in the lower TSF band was normalized to the maximum value obtained for that preparation. This enabled comparison of modulatory effects across different reconstitutions that produced different amounts of functional hemichannel activity (i.e., fractions of liposomes with functional hemichannels). Where several preparations were used, normalized datasets were combined for each condition for calculation of means and standard errors.

Hemichannel uptake assay

Calcein (10 mM stock) was prepared in “low calcium buffer” (10 mM Tris, 120 mM NaCl, 5.6 mM KCl, 0.5 mM CaCl₂, 1 mM MgCl₂, and 11 mM glucose, pH 7.4). Semi-confluent monolayers (35 mm²) were washed (10 mM Tris, 90 mM NaCl, 30 mM KCl, 2 mM CaCl₂, 1 mM MgCl₂, and 11 mM glucose, pH 7.4) and, to assess dye uptake, cells were incubated for 30 min at 37°C with “loading buffer” (100 μ M dye in 10 mM Tris, 120 mM NaCl, 30 mM KCl, 0.5 mM CaCl₂, 1 mM MgCl₂, and 11 mM glucose, pH 7.4). After 30 min, cells were washed with “normal buffer” (10 mM Tris, 120 mM NaCl, 5.6 mM KCl, 2 mM CaCl₂, 1 mM MgCl₂, and 11 mM glucose, pH 7.4) for dye imaging under a photomicroscope

(Axiovert 100; Carl Zeiss). Hemichannel uptake was assayed by counting the number of cells receiving dye from the extracellular solution (Quist et al., 2000). The results of each experimental condition with taurine were normalized to its own control experiment without taurine, which controls for differences in dye uptake as a result of potential differences in levels of plasma membrane hemichannel activity or levels.

"Parachute" assay for gap junctional communication

Semi-confluent "donor" and "receiver" cell populations were simultaneously induced for connexin expression by dox treatment for 48 h. The donor cells were then labeled with 10 μ M CM-DiI (stock 10 mM in DMSO) and 5 μ M calcein-AM (stock 5 mM in DMSO) for 30 min at 37°C. Donor cells were washed twice with 0.1 M PBS, pH 7.4, containing 0.3 mM glucose, trypsinized, seeded onto a semi-confluent monolayer of unlabeled receiver cells at an \sim 1:150 donor/receiver ratio, and then allowed to attach for 3 h at 37°C. Cells were examined and photographed under a photomicroscope (Axiovert 100; Carl Zeiss). Gap junction communication was assessed as the number of unlabeled cells receiving calcein (green) from each CM-DiI-labeled cell (red [+ green = yellow]). For each experimental condition, the average number of receiver cells containing dye per donor cell was determined and normalized to that of control cultures (Goldberg et al., 1995).

Molecular modeling

Molecular models of taurine and different Cx26-based peptides were made using Spartan 04 (Wavefunction, Inc.). Energy-minimized conformations were determined using MMFF94 force field rules (Halgren, 1996). If applicable, Hartree-Fock 6-31G* *ab initio* models (Hehre, 1973), subject to the MMFF-94 geometry constraints, were used for predicting molecular orbital structure (0.002 Å³/atomic unit) and chemical behavior, allowing electrostatic potential and local ionization potential to be mapped onto orbital surfaces.

Peptide synthesis

Peptides corresponding to specific sequences of the CL domain of rat Cx26 (Cx26CL), as defined by the UniProt database (<http://www.uniprot.org/uniprot/P21994>) to be residues 99–139, were tested for their ability to interact with a peptide with sequence corresponding to the Cx26CT (residues 213–226). The Cx26CL was arbitrarily divided into overlapping peptide segments corresponding to the first 20 amino acids of the CL nearest TM2 (CL1; residues 99–119), the last 20 amino acids of the CL nearest TM3 (CL3; residues 120–139), and the middle 20 amino acids (CL2; residues 109–129; see Fig. 6 A). Peptides (>95% purity) were synthesized using Fmoc chemistry with an automated synthesizer (433; Applied Biosystems).

The recent crystal structure of human Cx26 (Maeda et al., 2009) describes the CL as residues 98–129, whereas boundaries based on a combination of biochemical and hydrophobicity data are 97–132 (Nicholson, 2003; Sosinsky and Nicholson, 2005). The actual boundaries of functional, membrane-inserted channels remain uncertain. The rat and human Cx26 cytoplasmic domains are nearly identical in amino acid sequence.

Amino-terminal biotinylation of Cx26CL peptides (^{biot}Cx26CL) was through amino-terminal linkage of activated Lys-biotin by Fmoc-aminocaproic acid. Peptides were purified by C₁₈ reverse-phase HPLC using a Dionex DX500 system and assessed by electrospray-mass spectrometry using a Waters nano-liquid chromatography-coupled electrospray ionization quadrupole-TOF-MS.

For NMR, a peptide corresponding to the entire Cx26CT (AnaSpec) was further purified using a C₁₈ Sep-Pak cartridge (Waters) according to the manufacturer's instructions to remove salt and/or trifluoroacetic acid, present as a result of the synthesis

process, which might affect peptide resonance peaks during subsequent experiments. The peptide was eluted from the cartridge with acetonitrile and lyophilized.

Purification of the Cx26 CL peptide from *Escherichia coli*

Rat Cx26CL, residues 99–139, was subcloned into a *pet14b* vector (EMD), providing an amino-terminal (His)₆ tag and thrombin cleavage site, each separated by short linker sequences (HHHHHHH-SSG-LVPR-GSHM-Cx26CL), using flanking EcoRI and BamHI sites. *E. coli* strain BL21 (DE-3; EMD) transformed with the *pet14b*-Cx26CL was grown in M63 minimum media using 1 μ g [¹⁵N]H₄. Bacteria (0.6 OD₆₀₀) were induced with 0.5 mM isopropyl- β -D-thiogalactopyranoside (for 4 h at 37°C) and pelleted at 3,500 *g*_{av} (for 20 min at 4°C). Bacteria, resuspended in 0.1 M PBS, pH 7.4, containing Complete Protease Inhibitor (Roche) and 1 mM dithiothreitol, were lysed three times by French press. Debris was removed by centrifugation (3,500 *g*_{av} for 10 min at 4°C), and inclusion bodies containing His-tagged Cx26CL were collected by further centrifugation (25,000 *g*_{av} for 1 h at 4°C). The pellet was washed by centrifugation three times with 8 M urea, pH 8.0, and then resuspended in 5 M guanidine and 2 mM β -mercaptoethanol, pH 8.0. The solution was filtered (0.22 μ m) and loaded onto an affinity chromatography column (HisTrap HP; GE Healthcare), and the bound Cx26CL was washed with 100 mM imidazole and 5 M guanidine buffer, pH 8.0, before being eluted with 1 M imidazole and 5 M guanidine, pH 8.0, and dialyzed/precipitated against 20 mM MES, 50 mM NaCl, and 1 mM EDTA, pH 7.0. For NMR titration experiments, the Cx26CL was suspended in this buffer containing 6% LPPG. An intact purification tag and LPPG were necessary to maintain the solubility of the Cx26CL because of its preponderance of hydrophobic residues.

CT+CL peptide-binding assay

To assess interaction between Cx26CT and each of three ^{biot}Cx26CL peptides, and any effect of taurine, Cx26CT peptide (50 ng/ μ l or 100 ng/ μ l in 0.5 \times PBS at pH 6.5, 7.4, or 8.0; 100 μ l) was adsorbed in individual wells of a 96-well Immulon-1B plate (Thermo Fisher Scientific) for 24 h at 4°C. BSA (1% wt/vol in 0.5 \times PBS at pH 6.5, 7.4, or 8.0) was used as a control and also to block wells containing Cx26CT for a further 24 h at 4°C (200 μ l). After block, plates were washed with 200 μ l 0.5 \times PBS at pH 6.5, 7.4, or 8.0 containing 0.05% vol/vol Tween 20 (PBST). PBST containing various concentrations of ^{biot}Cx26CL synthetic peptides (up to 100 μ M) were added to wells (pH 6.5, 7.4, or 8.0; 100 μ l) for 3 h at 25°C in the presence and absence of taurine. After incubation, wells were washed (in PBST; pH and taurine concentration held constant), and 100 ng streptavidin-horseradish peroxidase (in PBST; pH and taurine concentration held constant) was added for 1 h. After further washing (in PBST; pH and taurine concentration held constant), the CT+CL interaction was assessed using an ELISA peroxidase substrate (200 μ l; 1-step 2,2'-azino-bis(3-ethylbenzthiazoline-6-sulfonic acid reagent [ABTS]; Thermo Fisher Scientific) incubated at room temperature for 30 min. Absorbance (405 nm) in each well was measured with a plate reader (Victor3; PerkinElmer) and interpreted as the concentration of ^{biot}Cx26CL noncovalently bound to Cx26CT.

NMR spectroscopy

NMR data were acquired on an NMR spectrometer (600 MHz; INOVA; Varian) using a cryoprobe. Interaction experiments between taurine and a 14-amino acid Cx26CT peptide were performed at pH 6.5, 25°C, and in 0.5 \times PBS; Cx26CT was 4 mM and taurine was 30 mM (1:7.5 molar ratio), or 1 mM taurine and 3 mM Cx26CT (1:3 molar ratio). Interaction experiments between taurine, Cx26CT, and Cx26CL were performed at pH 7.0, 42°C, in either 0.5 \times PBS or 20 mM MES, 50 mM NaCl, 1 mM EDTA, and 6% wt/vol LPPG; titrations from the Cx26CT point of view were

performed with 2 mM peptide in 0.5× PBS; titrations from the Cx26CL point of view were performed with 10 μ M peptide in 20 mM MES, 50 mM NaCl, and 1 mM EDTA containing 6% LPPG. Gradient-enhanced 2D ^1H - ^{13}C HMQC and 2D ^1H - ^{15}N HSQC were used to observe all natural carbon and nitrogen resonances.

RESULTS

Taurine effect on hemichannels is blocked by a purification tag on the Cx26CT

AS (taurine) effects on the activity of hemichannels composed of Cx26 and/or Cx32 were assessed by TSF, a robust liposome-based assay for large molecule permeability of channels (Harris et al., 1992; Rhee et al., 1996; Bevens et al., 1998; Bevens and Harris, 1999; Kim et al., 1999; Bao et al., 2004; Locke et al., 2004a,b; Tao and Harris, 2004, 2007; Ayad et al., 2006). TSF fractionates liposomes containing channels into discrete populations within an iso-osmolar density gradient, based on channel permeability to urea/sucrose. A change in liposome distribution between the uppermost and lowest band positions, relative to control, is a measure of a change in the fraction of hemichannels permeable to the gradient solutes. Such a change can be due to complete pore block or from reduction to near zero channel open probability.

Hemichannels were purified for functional study from HeLa cell lines stably transfected to inducibly express CT epitope-tagged Cx26 (Cx26_T), Cx32 (Cx32_T), or hemichannels containing both connexins where one

was tagged (Koreen et al., 2004; Locke et al., 2005). The epitope tag thus enabled recovery of homomeric Cx26_T and Cx32_T hemichannels and heteromeric Cx26_T/Cx32 and Cx26/Cx32_T hemichannels. Hemichannels were reconstituted into unilamellar liposomes, and the effect of AS (10 mM of protonated taurine) was assessed in TSF gradients (Fig. 1).

Previous studies showed that homomeric Cx26 and heteromeric Cx26/Cx32 hemichannels from native sources (i.e., untagged) were inhibited by protonated AS, and native homomeric Cx32 hemichannels were taurine insensitive (Rhee et al., 1996; Bevens and Harris, 1999; Locke et al., 2004b; Tao and Harris, 2004). Homomeric Cx32_T hemichannels were also taurine insensitive. Heteromeric hemichannels in which the Cx26 was untagged (Cx26/Cx32_T) were inhibited by AS, as were the native Cx26/Cx32 hemichannels. In contrast, hemichannels in which the Cx26 was tagged, whether heteromeric Cx26_T/Cx32 or homomeric Cx26_T, were not AS sensitive (Fig. 1 A). These hemichannels were not inhibited with up to 50 mM of protonated taurine. Thus, the presence of the CT tag on Cx26, whether in homomeric or heteromeric hemichannels, blocked the AS inhibition.

The CT epitope tag is linked to the connexin by a thrombin cleavage site. To explore the role of the tag per se on AS sensitivity, it was cleaved with thrombin before reconstitution. Tag cleavage (τ_c) is not blunt, leaving four additional amino acids (LVPR) at the carboxyl terminus of the thrombin recognition site) at the carboxyl terminus.

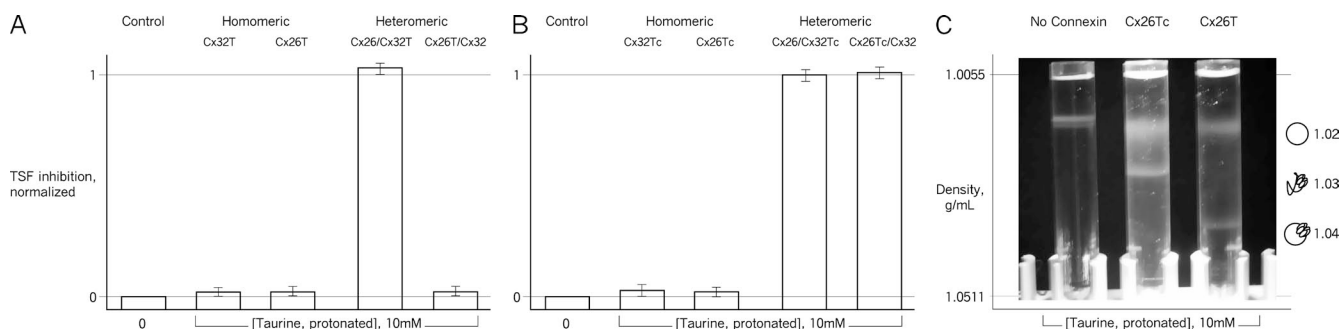


Figure 1. Taurine inhibition involves the CT of Cx26. Hemichannel activity in liposomes is assessed as permeability to urea/sucrose by TSF. (A) Effect of the AS taurine on activity of carboxyl-terminal epitope-tagged (_T) homomeric (Cx32_T and Cx26_T) and heteromeric (Cx26/Cx32_T and Cx26_T/Cx32) hemichannels. Only heteromeric hemichannels in which the Cx26CT is not tagged were AS sensitive; a tag on Cx26CT eliminated the AS sensitivity of homomeric Cx26_T and heteromeric Cx26_T/Cx32 hemichannels. Previous work showed that wild-type (untagged) Cx26-containing hemichannels were AS sensitive, and that homomeric Cx32 hemichannels were not (Bevens and Harris, 1999; Locke et al., 2004b; Tao and Harris, 2004). In this and subsequent TSF figures, the results for each experimental condition with taurine were normalized to its own control experiment without taurine ($n = 6-9$). (B) Effect of tag cleavage (τ_c), which leaves four additional amino acids (LVPR) at the carboxyl terminus, on sensitivity to AS. Cleavage restores inhibition to heteromeric Cx26_T τ_c /Cx32 hemichannels. AS sensitivity of all other hemichannel compositions was unaffected by tag cleavage. Surprisingly, the activity of homomeric Cx26_T τ_c hemichannels was unaffected by AS ($n = 5-8$). (C) AS narrows rather than closes Cx26_T τ_c hemichannels. In TSF, liposome permeability to urea but not sucrose forms a band of intermediate density. (Left to right) TSF gradients with liposomes formed in the absence of connexin (showing upper band only), liposomes containing Cx26_T τ_c hemichannels, and liposomes containing Cx26_T hemichannels, all exposed to 10 mM AS. For Cx26_T τ_c , the lower band density is shifted upwards compared with Cx26_T hemichannels. Therefore, AS narrows rather than closes Cx26_T τ_c hemichannels but has no effect on activity in TSF (B) or permeation (C) of Cx26_T hemichannels. None of the other channel compositions (tagged or tag-cleaved) was affected in this way by gradient AS. In A and B, the error bars are standard errors of the mean.

AS inhibition was restored in tag-cleaved heteromeric hemichannels (Cx26_{Tc}/Cx32), but, surprisingly, homomeric Cx26_{Tc} hemichannels remained AS insensitive (Fig. 1 B). Not surprisingly, the Cx32_{Tc} hemichannels were AS insensitive (see below), and Cx26/Cx32_{Tc} hemichannels were AS sensitive. Therefore, for heteromeric channels, the presence of the intact CT epitope tag but not the extra four amino acids that remain after tag cleavage interfered with AS inhibition, confirming the role of the CT tag in AS insensitivity and suggesting that the CT is involved in processes that occlude the Cx26 permeability pathway. However, in the homomeric Cx26_{Tc} hemichannels, the presence of the four additional amino acids was sufficient to block the AS effect on hemichannel activity.

Taurine narrows Cx26_{Tc} pores

TSF reports hemichannel activity as assessed by permeability to urea and sucrose (see Materials and methods). However, it is also possible that an applied compound restricts the pore diameter so that it is permeable only to the smaller molecule (i.e., urea, ~3.6-Å diameter) and impermeable to the larger molecule (i.e., sucrose, ~4.5-Å diameter). In this case, liposomes undergo osmotically driven shrinkage that results in a band of

intermediate density in TSF gradients (Locke et al., 2004a). Elimination of permeability to molecules as small as urea would effectively eliminate the ability of connexin channels to mediate molecular signaling *in vivo*.

To assess this possibility for Cx26_T and Cx26_{Tc} channels, densities of liposome bands were measured after TSF centrifugation. In taurine, the lower band of Cx26_T liposomes was at the same density as that of Cx26_{Tc} liposomes not exposed to taurine, indicating hemichannel permeability to both urea and sucrose. In contrast, in taurine the lower band of Cx26_{Tc} liposomes was at a less dense, intermediate position, indicating permeability of Cx26_{Tc} hemichannels to urea but not sucrose. Therefore, AS narrows rather than closes Cx26_{Tc} hemichannels (Fig. 1 C) and has no discernable effect on the pore diameter of Cx26_T hemichannels. Taurine-exposed liposomes containing tagged and tag-cleaved heteromeric Cx26/Cx32 and homomeric Cx32 hemichannels (Cx26_{T>Tc}/Cx32, Cx26/Cx32_{T>Tc}, and Cx32_{T>Tc}) do not form intermediate bands that indicate hemichannel narrowing; with AS treatment, liposomes containing untagged heteromeric Cx26/Cx32 hemichannels and homomeric Cx26 hemichannels change their distribution from the lowest band to the upper band,

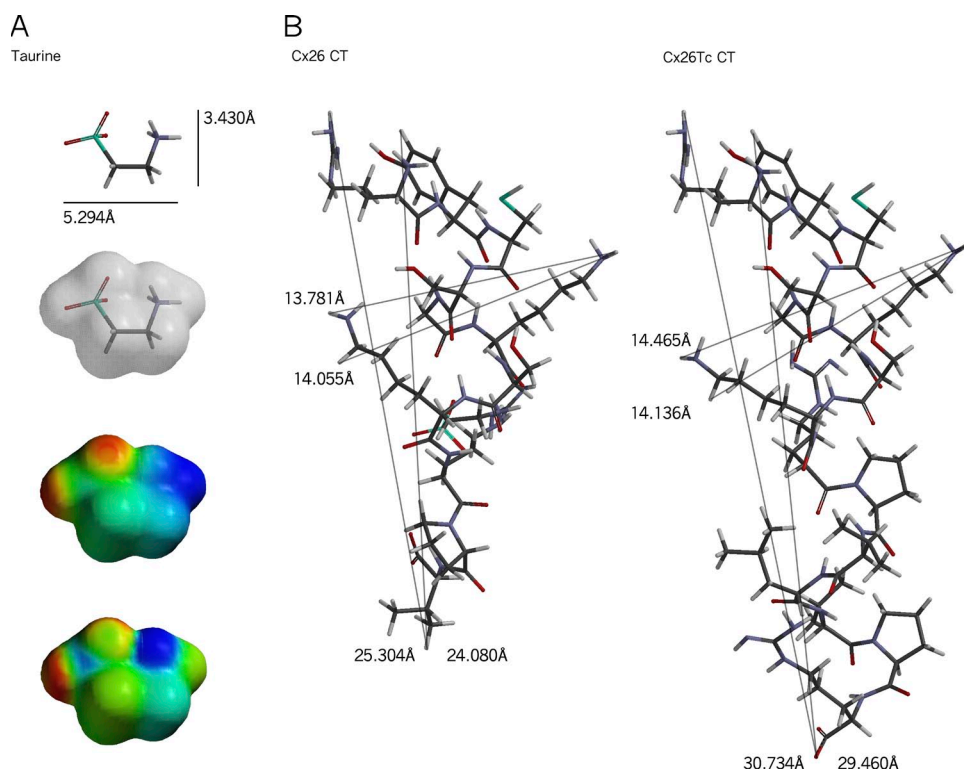


Figure 2. Cx26CT domain is involved in inhibition by taurine. The protonated amine of the AS is involved in connexin binding, and the ionized sulfonate moiety is involved in effecting the inhibition (Tao and Harris, 2004). (A) Side view of taurine showing the energy-minimized conformation determined using the MMFF94 force field rule. Black, carbon; red, oxygen; gray, nitrogen; blue, sulfur. (Below) Its molecular orbital structure (0.002 Å³/atomic unit; transparency) determined by Hartree-Fock 6-31G* *ab initio* models, subject to MMFF94 equilibrium geometry constraints; electrostatic potential (red, negative; blue, positive) and local ionization potential (red, ionized; blue, nucleophile) were mapped onto this orbital surface. (B) Energy-minimized conformations, in scale with A, of wild-type (nontagged) Cx26CT (left) and Cx26_{Tc} CT (right), as determined using the MMFF94 force field rule. Note two surface side-facing acidic lysine residues (K231 and K233), which may interact with the sulfonate group of taurine and/or be involved in pore occlusion.

not to an intermediate band, indicating full occlusion of the hemichannels.

Thus, there is an effect of AS on pore diameter only in homomeric Cx26 hemichannels with four extra amino acids at the carboxyl terminus. It is tempting to suggest that this AS-induced effect of a truncated tag on Cx26 is a partial form of the same molecular mechanism by which an untagged CT causes full occlusion of the pore in the presence of AS.

Subtle conformational differences between native Cx26 CT and Cx26_{TC} CT

TSF hemichannel studies implicate the Cx26CT in the AS effect on heteromeric Cx26-containing channels and in the AS-mediated narrowing of Cx26_{TC} hemichannels. An energy-minimized conformation for nontagged Cx26 CT and length-modified Cx26_{TC} CT was calculated using MMFF94 force field molecular mechanics (Halgren, 1996) (Fig. 2 B). In energy-minimized conformations, the Cx26_{TC} CT is ~5 Å longer than the nontagged (wild-type) Cx26 CT, but of similar width (K231–K233 distance measured in Fig. 2 B). If the CT acts by physically occluding the Cx26 pore, the difference in dimension of Cx26_{TC} CT could produce only partial or imperfect occlusion of the permeability pathway, resulting in permeability to urea but not sucrose, as observed in TSF.

Taurine affects hemichannel function in cells

The presence of nonjunctional hemichannels in plasma membrane is well supported (Contreras et al., 2003; Sáez et al., 2005; Srinivas et al., 2006). Hemichannels activate in low $[Ca^{2+}]_{ex}$ (e.g., 0.5 mM), providing a selective pathway for uptake of extracellular molecule(s) (Koreen et al., 2004) and/or release of cytoplasmic molecules (e.g., ATP, prostaglandin; Harris, 2007; Schalper et al., 2009).

The molecular permeability and AS sensitivity of Cx26 and/or Cx32 hemichannels was assessed by uptake of an extracellular membrane-impermeant dye, calcein, in low $[Ca^{2+}]_{ex}$ with and without induction of connexin expression (see Materials and methods; Koreen et al., 2004) (Fig. 3). Calcein loading into uninduced cells was minimal (Fig. 3 A, top). When connexin expression was induced, almost all cells were loaded (Fig. 3 A, bottom). Under both conditions, uptake in the presence of high $[Ca^{2+}]_{ex}$ was minimal, comparable to that without connexin induction.

Cytoplasmic taurine levels in HeLa cells can be modulated via extracellular taurine, which enters via an endogenous taurine transporter (Ramamoorthy et al., 1994). Extracellular taurine also may enter cells through non-junctional hemichannels opened by low $[Ca^{2+}]_{ex}$. Taurine modulation of low $[Ca^{2+}]_{ex}$ calcein uptake by cells expressing the different tagged connexin hemichannels was assessed. Uptake without induction of connexin expression was subtracted from that with induction, and the results normalized to uptake in the absence of taurine. Dye uptake was taurine sensitive only in cells expressing heteromeric hemichannels in which the Cx26 was untagged (Cx26/Cx32_T, not Cx26_T/Cx32) (Fig. 3 B). Dye uptake by these cells in the presence of taurine was markedly reduced compared with cells not exposed to taurine and compared with the absence of effect of taurine on uptake by the other cells under the same conditions. Thus, the taurine sensitivity of the various hemichannels expressed in cells corresponds to that seen with purified liposome-reconstituted hemichannels in the TSF system. The inhibition of dye uptake was not complete, which is likely to be due to differences in the cellular uptake of extracellular taurine and the intracellular levels achieved.

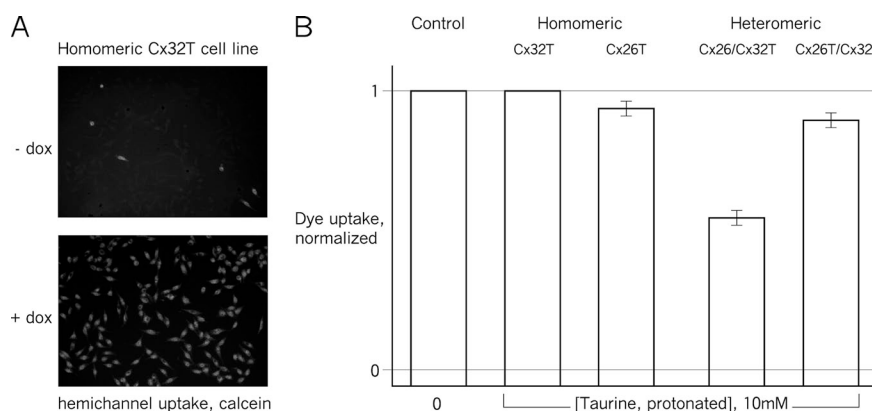


Figure 3. Taurine inhibits cellular hemichannel function. Calcein uptake by cells expressing connexin hemichannels was assessed by incubation with extracellular calcein in low Ca^{2+} medium (Goldberg et al., 1995; Li et al., 1996). (A) Dye uptake correlated with doxycycline-induced expression of connexin (Cx32_T in this illustration). Similar induction of dye uptake was observed for all cell lines used ($n = 3$). (B) Effects of extracellular AS on dye uptake by cells expressing the various connexin channels (extracellular taurine enters cells via a taurine transporter; Ramamoorthy et al., 1994) ($n = 3$). Only channels in which the Cx26 subunits are not tagged were AS sensitive, corresponding to the results from the liposome-based TSF study (Fig. 1). The results for each experimental condition with taurine were normalized to its own control experiment without taurine. Error bars are standard errors of the mean.

Taurine affects junctional channel function

The question arises as to whether taurine modulates the function of junctional channels in a manner similar to its effects on hemichannels. It is possible that the taurine-binding/effector site is inaccessible when hemichannels dock to form a junctional channel, or that the junctional structure itself does not permit the changes in pore structure that alter molecular permeability.

Gap junctions are permeable to large molecular weight dyes, used as indicators of junctional channel function (Weber et al., 2004). In our experiments, a donor–receiver parachute coupling assay was used to reveal changes to intercellular dye permeability in the presence of extracellular taurine. In brief, dye donor and receiver cells were preinduced for connexin expression. After induction, donor cell membranes were fluorescently labeled, and the cells were loaded with the junction permeable dye calcein (via its AM-ester). After removal of extracellular calcein-AM, donors were seeded onto a receiver cell monolayer, which was evaluated for calcein transfer from loaded to unloaded cells (Goldberg et al., 1995).

Intercellular dye transfer in taurine-exposed Cx32_T cells was unchanged compared with controls, as expected. Intercellular calcein transfer in taurine-exposed Cx26-expressing cells was decreased only in the Cx26/Cx32_T cells and not in the Cx26_T/Cx32 cells or the Cx26_T cells, compared with the same cells without taurine (Fig. 4 A). These results correspond to those seen in the studies of hemichannel liposomes and native membranes, above.

HEPES, a membrane-impermeant AS, was used to block cytoplasmic taurine uptake via its plasma membrane transporter (Petegnief et al., 1995). In the presence of extracellular HEPES, Cx26/Cx32_T junctional channels were AS insensitive in the presence of extracellular taurine (Fig. 4 A, arrow). Under these conditions of normal $[Ca^{2+}]_{ex}$, nonjunctional hemichannels are closed, so possible taurine influx through this pathway would be dramatically reduced. This result also shows that the taurine effect requires AS import into the cell, confirming the cytoplasmic location of its site of action, as suggested by the effects of the CT epitope tag.

Taurine closes nontagged Cx26 hemichannels and junctional channels

AFM and TSF studies have shown that purified nontagged homomeric Cx26 hemichannels close in response to acidification, but only in the presence of a protonated AS buffer (Locke et al., 2004b; Tao and Harris, 2004).

To directly assess AS sensitivity of nontagged Cx26 hemichannels and junctional channels in native membranes, cellular studies were performed using the HeLa cell line used for the previous AFM studies (Hand et al., 2002; Yu et al., 2007). The addition of taurine markedly reduced nontagged Cx26 hemichannel calcein uptake and junctional cell–cell passage of calcein, compared with the same cell lines without exposure to taurine (Fig. 4, B and C). Extracellular HEPES restored AS insensitivity to the nontagged Cx26-junctional channels in the presence of taurine (Fig. 4 C, arrow).

Collectively, these data make clear that AS modulates hemichannels and junctional channels that contain

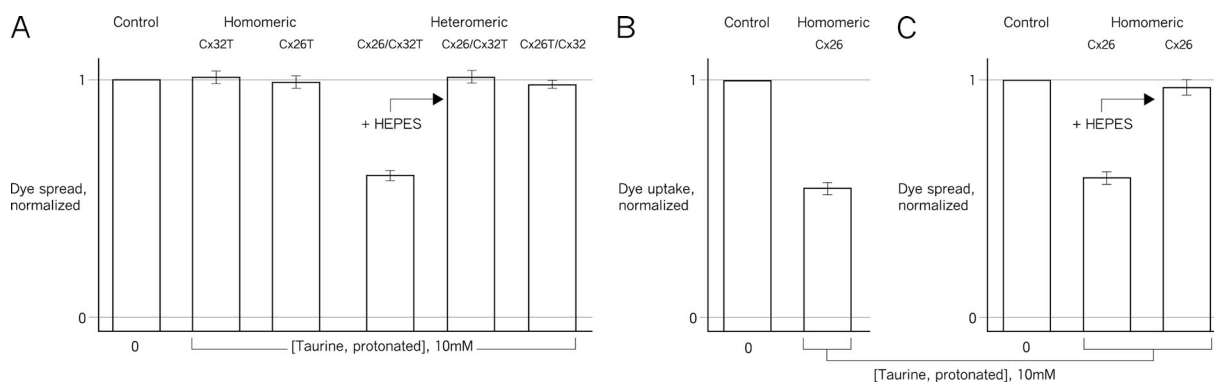


Figure 4. Taurine inhibition of gap-junctional channels and involvement of the CT. Intercellular spread of calcein was assessed by a “parachute” assay in which calcein-loaded donor cells were seeded onto a monolayer of receiver cells (Goldberg et al., 1995). (A) Only junctional channels in which the Cx26 subunits were not tagged were inhibited by extracellular AS, consistent with the hemichannel data (Figs. 1 and 3). A membrane-impermeant AS, HEPES, was used to block taurine transport into the cells (Petegnief et al., 1995). HEPES effectively eliminated the taurine effect on Cx26/Cx32_T junctional channel permeability of calcein ($n = 4-9$). (B) AS blocks wild-type (nontagged) Cx26 hemichannels. Hemichannel uptake of extracellular calcein was assessed as in Fig. 3. In contrast to the AS insensitivity of Cx26_T and Cx26_{TC} hemichannel function, nontagged Cx26 hemichannels were AS sensitive, as had been shown for preparations of purified hemichannels (Locke et al., 2004b; Yu et al., 2007), but not previously in a cellular context ($n = 3$). (C) AS substantially reduced intercellular calcein dye transfer through junctional channels composed of untagged Cx26, in contrast to no effect on Cx26_T junctional channels (see A; $n = 4-9$). The effect on nontagged Cx26-junctional channels was also eliminated by HEPES. The results for each experimental condition with taurine were normalized to its own control experiment without taurine. Error bars are standard errors of the mean.

Cx26, and that the modulation critically involves the CT of Cx26, and does not involve Cx32.

Taurine does not bind Cx26CT

The Cx26CT domain contains no acidic residues, that is, residues that could interact electrostatically with the amine group of AS, except for the carboxyl terminus itself. However, the Cx26CT contains several basic residues that could interact with the sulfonate moiety of AS. An electron density model of taurine (i.e., van der Waal surface of its energy-minimized structure) was calculated using the *ab initio* Hartree–Fock self-consistent field method (Hehre, 1973), allowing electrostatic potential and local ionization potential to be mapped onto its orbital surface (Fig. 2 A). In energy-minimized conformations, there are two surface side-positioned, outward-facing basic lysine residues (positions K231 and K233) in Cx26CT and Cx26_{TC} CT structures that could interact with the taurine sulfonate group (Fig. 2 B, in red on taurine potential surfaces).

The potential binding of AS to Cx26CT was explored by NMR. The ¹³C-HMQC spectrum obtained from a 14-residue peptide corresponding to the Cx26CT was overlaid with a spectrum from the same peptide in the presence of taurine (Fig. 5 A). Also, the ¹³C-HMQC spectrum from taurine was overlaid with that observed in the presence of the peptide (Fig. 5 B). In both cases, the centroids of the resonances were identical, indicating that taurine does not structurally interact with a peptide corresponding to the entire CT of Cx26.

pH-dependent intramolecular binding involving Cx26CT and Cx26CL is modified by taurine

The clear involvement of the Cx26CT and the absence of a binary interaction with taurine suggest that the CT and/or taurine interact with another connexin domain,

perhaps in a ternary complex, or that taurine competes with CT for a binding site on another connexin domain. An intramolecular complex involving the CT and CL domains of Cx26 had been postulated from previous work, based on superficial sequence homologies with taurine-binding sites of pentameric ligand-gated ion channels (Bevans and Harris, 1999; Tao and Harris, 2004). In addition, in other connexins there is interaction of CT and CL domains; pH gating of Cx43 channels involves interaction of the Cx43CT (“ball”) with a “receptor” domain in its CL (Cx43CL; Homma et al., 1998) (however, the Cx43CT is significantly longer than the Cx26CT, and the Cx26CT does not contain the sequences of the Cx43CT that its pH sensitivity requires).

The possibility of binary or ternary interactions among AS, Cx26CT, and Cx26CL was first assessed by peptide ELISA. Specifically, ELISA was used to test whether the Cx26CT peptide binds to the Cx26CL, to which regions, and whether this occurs in an AS-dependent or AS-independent manner. ELISA plates coated with Cx26CT peptide at 50 or 100 ng/μl were probed with each of three biotinylated Cx26CL (^{biot}Cx26) peptides at pH 6.5, 7.4, and 8.0. These CL peptides match the first 20 amino acids of the Cx26CL nearest the second transmembrane domain (TM2) (^{biot}CL1), the last 20 amino acids nearest the third transmembrane domain (TM3) (^{biot}CL3), or the middle 20 amino acids (^{biot}CL2) (Fig. 6 A).

The data show significant interaction only between the Cx26CT peptide and ^{biot}CL3, a peptide corresponding to the CT-proximal region of the Cx26CL, residues 120–139. The Cx26CT–^{biot}CL3 interaction increases with acidic pH. Furthermore, this interaction is substantially reduced by 10 mM taurine (Fig. 6 A; rightmost bar of each triplet). ^{biot}CL1 and ^{biot}CL2 did not bind immobilized Cx26CT at any of the pHs tested.

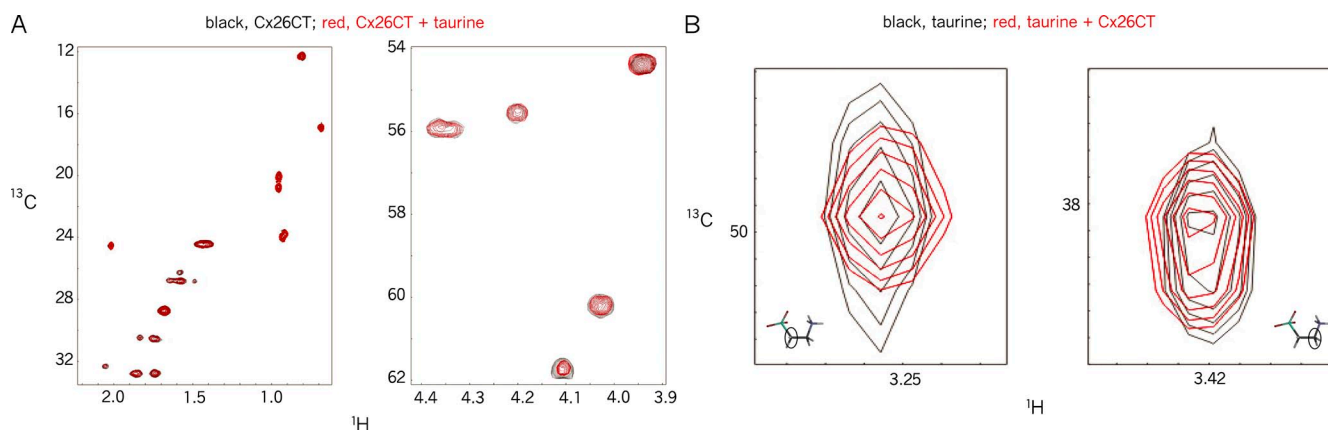


Figure 5. ¹³C-HMQC NMR demonstrating the Cx26 CT 14mer does not complex with taurine. (A) The spectrum of the Cx26CT alone (black) is overlaid with its spectrum in excess taurine (red) at a 1:7.5 molar ratio. The two overlays (left vs. right) differ in the proton region selected for observation. (B) Close-up of a spectrum of each of the two methyl (–CH₂) groups of taurine (black) overlaid with the same spectrum of taurine in excess Cx26CT (red) at a 1:3 molar ratio. (Left) The methyl group closest to the sulfonate moiety (–SO₃H). (Right) The methyl group closest to the amine (–NH₂). In both cases, the resonance centers do not change, which further indicates lack of interaction between taurine and the Cx26CT peptide.

Concentration dependence curves derived from the ELISA data for the Cx26CT-^{biot}CL3 interaction at pH 6.5 and 7.4 are shown in Fig. 6 B. The monoexponential increase in the amplitude of the binding to Cx26CT as a function of ^{biot}CL3 concentration suggests that this interaction is described by first-order kinetics, and accordingly, the apparent K_d s could be determined at each pH. The data show that the apparent affinity of the ^{biot}CL3 peptide for the Cx26CT was

greater at lower pH, consistent with Fig. 6 A. The dissociation constants are in the low micromolar range at pH 7.4. No difference in K_d was seen for the two concentrations of Cx26CT peptide used as bait (data in Fig. 6 B are pooled from 50- and 100-ng/ μ L experiments), also consistent with a first-order interaction. These data make clear that, for Cx26, acidic pH in the physiological range enhances interaction between its CT and a specific segment of the CL nearest TM3.

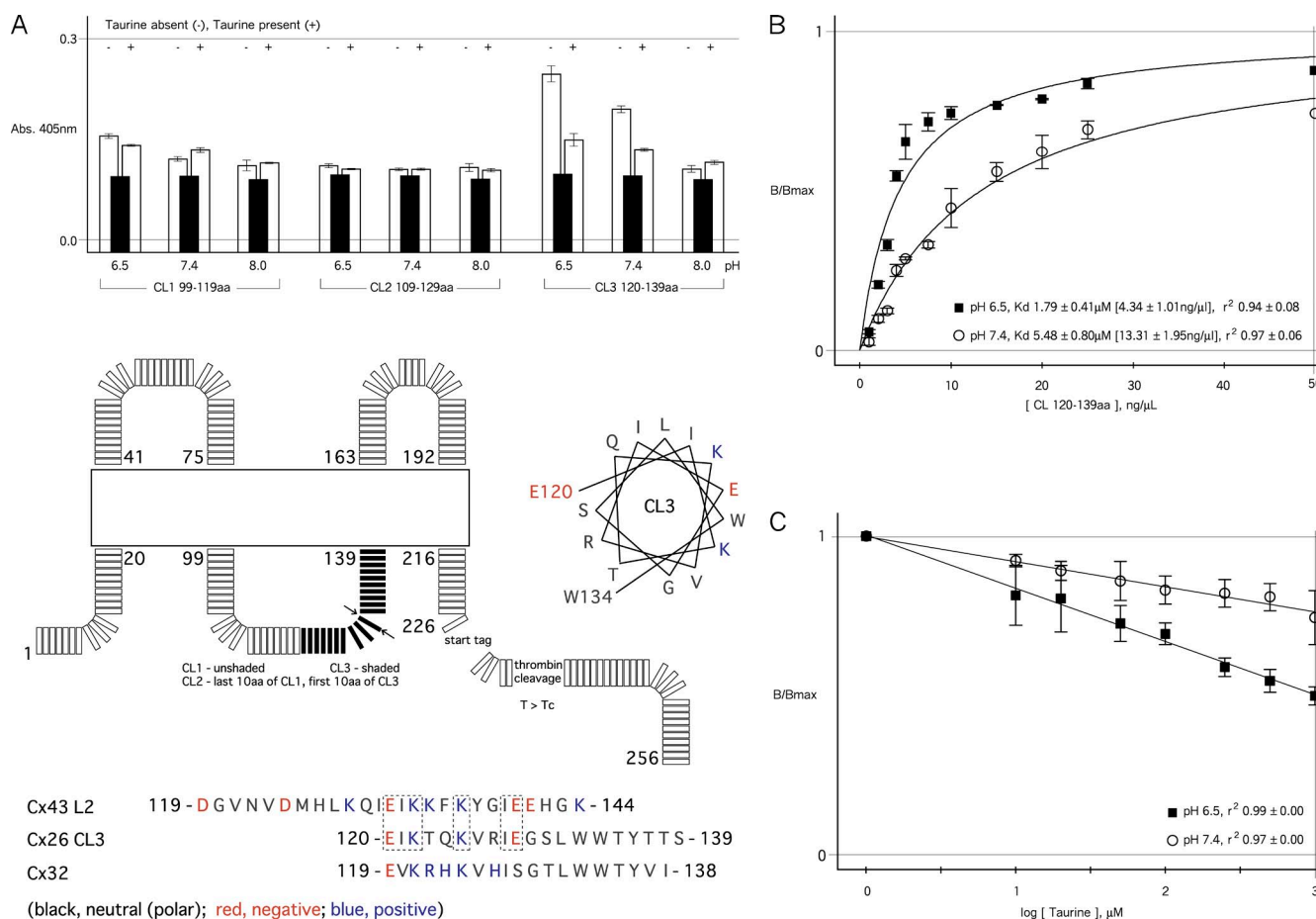


Figure 6. pH-dependent binding of Cx26CT to Cx26CL is modified by taurine. Interaction between the CT peptide and peptides based on the CL domain at different pHs, and the effect of taurine (absence [–] or presence [+]) on the interaction was assessed by a modified ELISA technique. A peptide corresponding to the entire Cx26CT was immobilized and used as bait. (A) pH-dependant interaction between Cx26CT and the second half of the Cx26CL (CL3) occurred at acidic pH and was largely reversed by taurine. In contrast, CL2 (peptide corresponding to the middle 20 amino acids of the Cx26CL) showed no significant interaction with the CT peptide, and although CL1 (peptide corresponding to the first 20 amino acids of the Cx26CL) showed some interaction at acidic low pH, this was unaffected by taurine. (Bottom) Schematic of the nonmembrane residues of rat Cx26, the positions of the three ^{biot}Cx26CL peptides used for the ELISA, and homology comparisons (black, neutral; red, negative; blue, positive) between ^{biot}CL3 and the corresponding segments in rat Cx32 and human Cx43. The CL-TM3 boundary of human Cx26 as shown by crystallography (Maeda et al., 2009) is identified by apposing arrows. The helical wheel representation of CL3 indicates an amphipathic character, with a strongly hydrophobic stripe (I, L, I), if it is α helical (the CL was unresolved in the crystal structure). (B) Fractional binding is plotted against the concentration of ^{biot}Cx26CL residues 120–139 (CL3) at pH 6.5 (filled squares) and pH 7.4 (open circles). Dissociation constants (K_d s) were determined from single-exponential fits to the data. (C) Fractional binding is plotted as a function of the log taurine concentration at pH 6.5 (filled squares) and pH 7.4 (open circles). Binding at 0 mM taurine is normalized to unity for each pH condition. Each data point is the mean of three independent experiments at 50 and 100 ng/ μ L of immobilized Cx26CT bait. In A and C, CL peptide concentration was 10 μ M. In A, taurine concentration was 10 mM, and filled bars are nonspecific interaction with BSA. No significant binding of any ^{biot}Cx26CL peptide was detected when BSA (1% wt/vol) was used as bait or ligand, when ^{biot}Cx26CL was added to uncoated plates, or plates were coated with 1% wt/vol BSA. Error bars are standard errors of the mean.

Intramolecular interactions have not been shown previously for Cx26.

The inhibitory effect of taurine on this pH-driven interaction is demonstrated in Fig. 6 C, which shows the effect of increasing taurine concentration on the interaction between the Cx26CT “bait” and a concentration of ^{biot}CL3 near its *K_d*s (10 μM; 6.26 ng/μl) at pH 6.5 and 7.4. Disruption of the interaction between the CL and CT peptides was a linear function of the log of taurine concentration over the range shown, and was substantially greater at the lower pH (i.e., the relation has a steeper slope). Approximately 50% of the CL–CT peptide interaction is disrupted at 1 mM taurine at pH 6.5. At taurine concentrations beyond 1 mM, the trend continued, with complete dissociation by ~5 mM, but the relations could not be fit to any standard binding isotherm, suggesting pleiotropic effects on the peptide structure/interactions at these concentrations that could not be mechanistically characterized.

Collectively, these binding studies demonstrate a specificity of Cx26CT–^{biot}CL3 interactions, with acidic pH both enhancing the interaction as well as the ability of taurine to disrupt it.

Taurine and Cx26 CT interact at some of the same sites on Cx26CL

The ELISA results suggested further NMR structural characterization of the Cx26CT and Cx26CL interactions, in the presence and absence of taurine. NMR spectra of the entire Cx26CL (10 μM) labeled with [¹⁵N]H₄ reveal interactions with taurine (30 mM) (Fig. 7 A) and the Cx26CT peptide (4 mM) (Fig. 7 B) at pH 7.0. The main resonance spectra show that both taurine and the Cx26CT affect many Cx26CL resonance peaks, but that more resonance peaks are affected by the Cx26CT than by taurine; for example, in Fig. 7, more resonance peaks show displacement of the red (with taurine or Cx26CT) from the black (control) spectra. Close-ups of individual resonance peaks in Fig. 7 show that taurine interacts with the Cx26CL at some residues (peaks iii and iv), but not at others at which the Cx26CT does (peaks v and vi). There are other resonance peaks at which there is no effect by either taurine or the Cx26CT (Fig. 7, peaks i and ii).

These NMR data confirm interaction between the Cx26CT and Cx26CL. They also indicate that an interaction site for taurine exists in the Cx26CL (as opposed

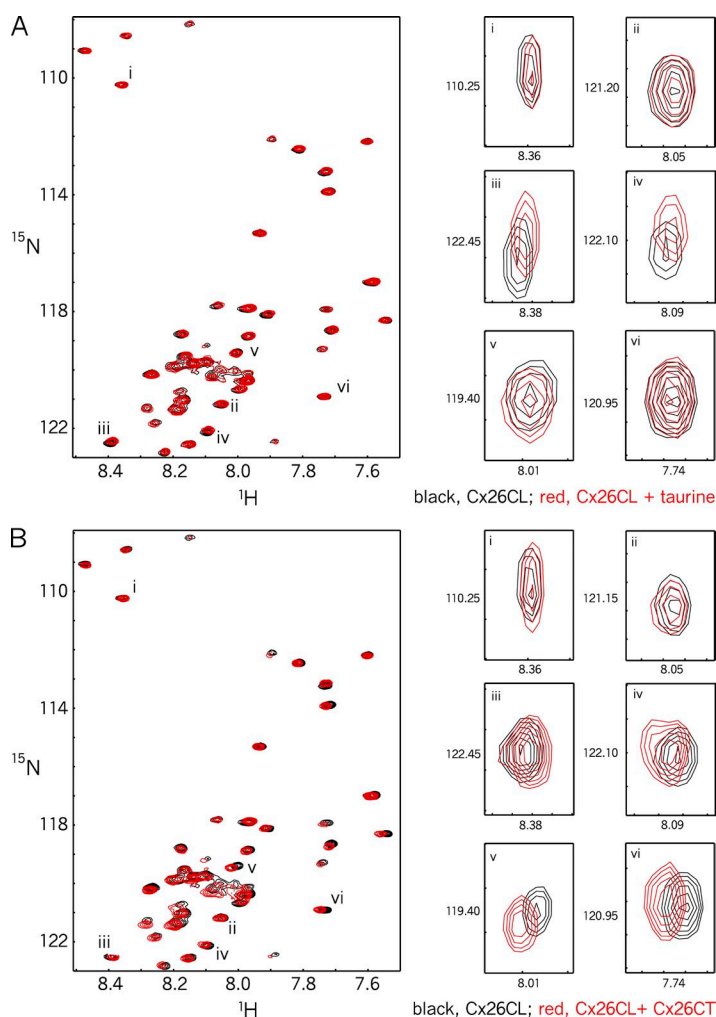


Figure 7. ¹H-¹⁵N HSQC demonstrating that Cx26CL interacts with both taurine and the Cx26CT. Pairwise interactions between CL peptide and taurine or CL peptide were reassessed by NMR. Control spectrum of the [¹⁵N]-labeled Cx26CL (10 μM; black) overlaid with spectra of the Cx26CL in the presence of (A) 30 mM taurine (red) or (B) 4 mM Cx26CT peptide (red). (Right) Close-up view of representative resonance peaks of the Cx26CL that were unaffected (i and ii) and affected (iii–vi) by the presence of these ligands. Resonance peaks iii and iv were affected by taurine, but resonance peaks v and vi were not, whereas resonance peaks iii–vi were affected by the Cx26CT peptide.

to the Cx26CT; Fig. 5), and that taurine affects only a subset of the Cx26CL residues that interact with the Cx26CT. This latter finding suggests that some sites of Cx26CT and taurine interaction with the Cx26CL overlap, providing a rationale for the disruption of the CL–CT interaction by taurine seen by ELISA.

The resonance spectra in Fig. 8 show the effect of taurine on Cx26CL–Cx26CT interactions as reported by changes in the resonances of [^{15}N]-labeled Cx26CL. First, there are residues (resonance peaks) in Cx26CL that are unaffected by interaction with the Cx26CT, both in the presence and absence of taurine, as indicated in Fig. 8 A by the absence of centroid displacement of the contours for Cx26CL alone (black), Cx26CL+taurine (red), Cx26CL+Cx26CT (blue), and Cx26CL+Cx26CT+taurine (green). Other resonance peaks in the Cx26CL are affected by the Cx26CT (displacement of black and blue contours) and unaffected by taurine (no displacement of red from black, or green from blue contours; Fig. 8 B).

Significantly, some Cx26CL residues affected by the Cx26CT (displacement of blue from red contours in Fig. 8 C) return back toward their Cx26CT-unbound state in the presence of taurine (superimposition of black and green contours), indicating that taurine reverses the Cx26CL–Cx26CT interaction at this position. At the same resonances, the addition of taurine alone affects the Cx26CL (displacement of red from black in Fig. 8 C), suggesting direct taurine interactions with the Cx26CL at the same sites (a binary interaction).

Thus, an interaction site for taurine exists in the Cx26CL, and taurine affects a subset of the Cx26CL residues that also can interact with the Cx26CT. Lastly, there are resonance peaks in the NMR spectra affected independently by taurine and by the Cx26CT, which move to unique positions in the presence of both taurine and the Cx26CT (Fig. 8 D). This could suggest that taurine interacts at unique sites generated by the Cx26CL–Cx26CT complex (a ternary interaction) or that the site has not been sufficiently saturated with taurine to disrupt the Cx26CL–Cx26CT complex so the observed changes in peak resonance result from a mixture of reversed and nonreversed Cx26CL–Cx26CT interactions (a mixture of binary interactions involving this site).

Collectively, these NMR data show direct binary interaction of taurine with the Cx26CL and direct binary interaction of the Cx26CT with the Cx26CL. They also show that some Cx26CL sites affected by taurine are also affected by Cx26CT. The addition of taurine can completely reverse the effect of Cx26CT binding at some sites, and at other sites may form a ternary complex under these conditions. At sites where taurine does not interact with the Cx26CL, it has no effect on the Cx26CL–Cx26CT interaction; only where taurine interacts with the CL does it have an effect on CT–CL interactions. A simple

but not necessarily complete scenario that emerges is that taurine can directly displace the CT from sites on the CL by binding at those CL sites; thus, taurine is a competitive inhibitor of the interaction between Cx26CT and the Cx26CL.

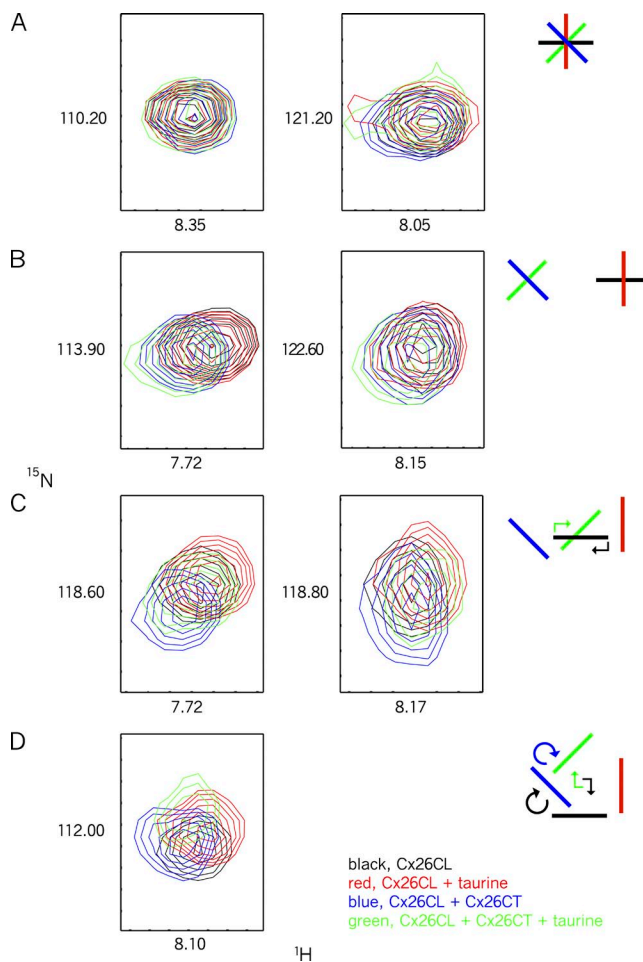


Figure 8. ^1H - ^{15}N HSQC demonstrating that the Cx26 CT–CL complex is affected by taurine. Interactions among CT peptide, CL peptide, and taurine were further assessed by NMR. All panels display individual Cx26CL resonance peaks. In each spectra, contours are colored as follows: black, [^{15}N]-labeled Cx26CL; red, [^{15}N]-labeled Cx26CL plus taurine; blue, [^{15}N]-labeled Cx26CL plus unlabeled Cx26CT; green, [^{15}N]-labeled Cx26CL plus unlabeled Cx26CT plus taurine. Concentrations are as follows: 10 μM Cx26CL, 4 mM Cx26CT, and 30 mM taurine. (A) Resonance peaks of Cx26CL that are unaffected by taurine, by Cx26CT, or by both taurine and Cx26CT. (B) Resonance peaks of Cx26CL showing no effect of taurine (black and red overlap), an effect of the Cx26CT (blue displaced from black), and a negligible effect of taurine on the Cx26CL–Cx26CT complex (green superimposed on blue). (C) Resonance peaks demonstrating an effect of taurine on Cx26CL (displacement from red from black), an effect of Cx26CT on Cx26CL (displacement of blue from black), and, intriguingly, displacement of the Cx26CL–Cx26CT complex by taurine (green moves away from blue toward black). (D) Resonance peaks showing a site in Cx26CL that is affected differently by each of the conditions (none of the spectra overlap).

DISCUSSION

Previous work showed that protonated AS act directly on channels that contain Cx26 to inhibit their permeability. The present work shows that the AS effects require an unmodified CT and explores the mechanism of AS inhibition using wild-type Cx26 and Cx26 with amino acid additions to the carboxyl terminus, when expressed as homomeric channels and as heteromeric channels with wild-type Cx32 and with Cx32 with amino acid additions to its carboxyl terminus.

The AS-mediated inhibition was studied using hemichannels reconstituted into liposomes, hemichannels in plasma membranes of cells, and junctional channels between cells. The results were consistent across all three systems, showing that the CT of Cx26 is a critical component of AS sensitivity and that the effect occurs only when AS has access to the cytoplasmic aspect of the channels.

ELISA and NMR studies showed that AS does not interact with the isolated Cx26CT, but rather that the CT can interact directly with the proximal segment of the complex, more so at acidic pH, and that AS interacts with the complex to disrupt this interaction, which correlates with inhibition of channel function. These findings are interpreted in the contexts of the molecular and intramolecular interactions involved and of the proposed gating mechanisms of connexin channels.

Involvement of the Cx26CT

The liposome data show that for homomeric Cx26 channels, an unmodified CT is required for AS-mediated inhibition, which does not require other soluble/cytoplasmic factors or involvement of other connexins. The addition of four extra amino acids to the CT (Cx26_{TC}) converts the effect of AS from pore occlusion to pore narrowing, whereas a longer (28-amino acid) extension to the CT (Cx26_T) eliminates the AS effect completely. These results suggest that the CT is a crucial component of AS-mediated effects of Cx26 on channel function, and that AS itself does not occlude the pore. This is the first evidence that the short Cx26CT influences channel function.

Thus, all indications are that the CT of Cx26 itself is directly involved in the subsequent AS channel inhibition. It follows that the Cx26CT could be the locus of AS binding and/or be structurally involved in channel gating. The narrowing of the channel in response to AS when there is a minor length alteration (LVPR sequence at the carboxyl terminus; Cx26_{TC}) suggests direct involvement of the CT in Cx26 pore occlusion.

AS–CL interactions

In theory, the AS-binding site could be within the Cx26CT, or elsewhere with allosteric involvement of the CT. NMR studies answered this question, showing that there was no

detectable interaction of taurine with a peptide corresponding to the full-length CT (Fig. 5), but that there was interaction between the full-length CL and taurine. Furthermore, the NMR studies revealed interactions between the CL peptide and the CT peptide, and that taurine interfered with this interaction (Figs. 7 and 8). These data identify AS as a modulator of CL–CT interactions. The specificity and characteristics of these interactions were explored by ELISA, which showed that the CT interacted only with the second half of the CL, this interaction was favored by low pH, and taurine disrupted it by competitive interaction (Fig. 6).

As mentioned, previous work showed that the protonated amine of AS is a key element of binding to connexin, and that the sulfonate moiety is involved in the functional effect (Tao and Harris, 2004). The first half of the CL3 peptide (rat Cx26, residues 120–129) contains a mixture of positive and negative charged residues, providing opportunity for interaction with both charged moieties of taurine (Fig. 6 A). The pH- or AS-dependent gating of human Cx26 channels that have mutations in this segment have not been reported, although mutations at K122 or R127, or deletion of E120, are reported to cause nonsyndromic deafness in humans (Green et al., 1999; D'Andrea et al., 2002; Palmada et al., 2006; Mani et al., 2009). Mutation at the latter two sites yields channels that insert in plasma membrane but do not mediate junctional coupling.

The recent crystal structure of human Cx26 (Maeda et al., 2009) shows the CL/TM3 (third transmembrane domain) boundary at residue 129, whereas biochemical/hydrophobicity data show it at residue 132 (Nicholson, 2003). The actual boundary in functional membrane-inserted channels remains uncertain, but in either case, the region of charged residues that potentially interact with the Cx26CT and/or AS in the first half of the Cx26CL3 peptide would be that immediately proximal to TM3, a region perhaps close to the Cx26CT (the crystal structure did not resolve the CL or the CT).

Comparison of the corresponding sequence in the AS-insensitive connexin Cx32 shows that the Cx32 sequence lacks an acidic residue at position 128 (Cx26-E128 vs. Cx32-S128), which is very close to the hydrophobic second half of the sequence, which is proximal to TM3, and immediately follows a highly basic segment (Fig. 6 A). It is tempting to speculate that because AS action requires close coordination with both a basic and an acidic residue, the absence of the acidic residue at position 128 prevents an AS effect on Cx32 channels.

CL–CT interactions

NMR and the ELISA studies together make two important points about CL–CT interactions in Cx26: (1) there is an interaction, and (2) it is favored by mildly acidic pH. This is the first evidence for interdomain modulatory interactions in Cx26. Interaction between the CL

and CT and its involvement in channel gating have been demonstrated for Cx43 and several other members of the α family of connexins (Stergiopoulos et al., 1999) (<http://www.genenames.org/genefamily/gj.php>). This is the first demonstration of an intramolecular interaction between cytoplasmic domains for the β family of connexins, which in addition to Cx26 includes Cx25, Cx30, Cx30.3, Cx30.1, Cx31.1, and Cx32. It is somewhat unexpected that the CT of Cx26 would be involved in interdomain interactions and in gating, as it has been regarded as being too short to have regulatory effects.

The finding that in Cx26 the CL–CT interaction is favored by acidic pH allows for an intriguing comparison with pH gating in other connexins. In the previously described cases where a pH-driven CL–CT interaction has been established, all involving α connexins, this interaction closes the channel. In contrast, for Cx26 (a β connexin) it does not, but its disruption—in this case by AS—does. Furthermore, a cytoplasmic molecule, taurine, is necessary for the pH-dependent channel closure. Because other cytosolic AS, including L-cysteic acid, L-homocysteic acid, and hypotaurine, have similarly been shown to be effective modulators of Cx26-containing channels, there are likely to be other endogenous ligands for β connexin family members. Based on the AS-induced pore narrowing of Cx26_{TC}, we speculate that Cx26CT free of interaction with the CL adopts a conformation at low pH that leads to pore occlusion, either directly or allosterically. On the basis of the AS-induced disruption of the CL–CT peptide interaction in the ELISA data, we do not favor formation of a stable ternary complex between the CL, CT, and AS.

The molecular basis of the specific association between the Cx26CT peptide and the CL3 peptide is unknown; neither peptide contains histidine, whose protonation state on the basis of solution pK_a would be altered over the indicated pH range. However, solution pK_a s may not pertain; local microenvironment can dramatically modify pK_a s, bringing acidic or basic side-chain pK_a s into the neutral range (González-Nilo et al., 2002; Harris and Turner, 2002; Mukoyama et al., 2004). For example, a local hydrophobic environment, such as that in the second half of CL3 and the adjacent TM3, favors the uncharged form of titratable groups and can raise the pK_a of glutamate, the negative amino acid in CL3, by more than 2 pH units. Such modulation of pK_a s operates in pH sensing/sensitivity in other channels (Schulte et al., 1999; Seifert et al., 1999). The high concentration of charged residues in both the Cx26CL3 segment and the CT affords ample opportunity for such effects.

AS–CT–CL interactions

The NMR data show direct interaction between the Cx26CT peptide and the full-length Cx26CL peptide at pH 7.0. The ELISA data show an interaction between the Cx26CT peptide and only the ^{biot}CL3 peptide,

corresponding to the second half of the Cx26CL, proximal to TM3, which increases with pH change from 8.0 to 6.5. Although the peptides differ and the conditions are necessarily quite different, both types of experiments show interactions at corresponding pHs.

The NMR spectra in Fig. 8 indicate a variety of interactions at different sites in the Cx26CL. Specifically, the spectra in Fig. 8 C show complete reversal by AS of the effect of the CT on CL peak resonances, as expected for complete dissociation of the CT from the CL. However, the spectra in Fig. 8 B show no effect of AS at a site (resonance peak) where the CT has an effect, suggesting that the CL–CT interaction persisted. The spectra in Fig. 8 D show an intermediate condition, in which AS had an effect on the CT-induced shift but did not reverse it. The latter two categories indicate that in the conditions under which the spectra were obtained either (a) there was a ternary complex between all three elements, or (b) the displacement of the CT from the CL was incomplete. The ELISA data in Fig. 6 A indicate substantial but not complete dissociation of the CT peptide from the ^{biot}CL3 peptide at high taurine concentration, which could account for the heterogeneity in the NMR spectra. It could also indicate that AS interaction with the CL is positively modulated by formation of the CL–CT complex. The precise structural mechanism of AS-induced CT–CL dissociation remains unclear. Nevertheless, given that the dominant effect of AS is to both decrease the CL–CT interaction and increase the impermeability of the channels, we attribute the latter to the former, favoring a binary AS–CL interaction rather than a stable ternary AS–CL–CT interaction as responsible for the functional effect.

We also note the substantial differences in the conditions and peptides required for the two types of experiments of modular interaction. The NMR studies were performed in free solution with a His-tagged full-length CL peptide and the CT peptide, in 6% LPPG and pH 7.0 at 42°C (see Materials and methods). The ELISA studies were performed using immobilized Cx26CT peptide and a peptide corresponding to only part of the Cx26CL in 0.05% Tween 20 at 4°C. Despite these differences, the results tell a qualitatively self-consistent story. Unfortunately, attempts to lower the pH caused significant precipitation of the peptides at the concentrations required to obtain NMR spectra.

Proposed domain-level mechanism(s)

The ELISA studies show that AS disrupts the CL3–CT interaction. The NMR data show that AS binds to the CL only and provide further evidence that AS disrupts the CL–CT interaction. Collectively with the functional studies, these data suggest the following scenario. At normal pH, the Cx26CT and Cx26CL interact to some degree. As pH becomes acidic, the interaction between the CT and CL becomes stronger. With increasing

concentration of cytoplasmic AS, the CL–CT interaction is disrupted, which leads to channel closure. Channel closure could be effected by any of several consequences of the disruption of the CL–CT interaction. These include: (a) the free CT physically blocks the pore at low pH, but not at normal pH; (b) the free CT at low pH interacts with another connexin domain, which closes the pore directly or allosterically; (c) the CL at low pH, when free of interaction with the CT and interacting with AS, physically blocks the pore; and (d) the CL at low pH, free of interaction with the CT and interacting with AS, allosterically blocks the pore, alone or via interaction with another connexin domain.

If the CT is the active component (a and b above), the long addition to it (tag [T]) would render it unable to block the pore, directly or allosterically. Alternatively, the long addition could disable the ability of AS to disrupt the CL–CT interaction. The fact that the short addition (cleaved tag [T_C]) retains an AS effect (pore narrowing) argues most simply that, if the CT is the effective element, it directly occludes the pore, and that the short addition interferes with complete occlusion. One could imagine a less likely scenario of modulation by an allosteric effect, however. That an AS effect is retained with the small addition suggests that it does not interfere with the CL–CT interaction.

If the CL is the active component (c and d above), the long addition to the CT could disable the ability of AS to disrupt the CL–CT interaction or the ability of the free CL to effect pore closure. The short addition to the CT, which retains an AS sensitivity, could affect CL–CT complex formation but compromise direct or allosteric CL-mediated channel closure.

Put in other terms, the data suggest either that in wild-type proteins at low pH the CT is tied up by the CL so that it cannot cause channel closure unless AS is present, or that the CT ties up the CL so that it cannot close the channel unless AS is present.

Both scenarios involve two effects of acidic pH: structural effects on the CT and/or CL that enable pore occlusion, and the coordinated (and perhaps related) increase of their affinity of interaction so that this does not occur. The CT–CL interaction is dominant (keeping the channel open), unless disallowed by the presence of AS, in which case the channel is occluded.

Previous work had suggested two possible mechanisms: one in which a binary interaction between either AS or the CT interacted with a “receptor” domain (shown here to involve a segment of the CL closest to TM3) to close the channel, and one in which a ternary interaction between the AS, the CT, and the receptor domain closes the channel (Bevans and Harris, 1999). The present work reveals a mechanism that combines elements of both: the binary interaction of AS with the CL does not in itself close the pore, and neither does a ternary interaction. At acidic pH, a binary interaction of

the CL with the CT keeps the pore open, and either a binary interaction of the CT with the pore itself or an allosteric effect of the CT structure at acidic pH closes it.

Homomeric Cx32 channels are insensitive to AS, but heteromeric Cx26/Cx32, Cx26/Cx32_T, and Cx26/Cx32_{T_C} channels are AS sensitive, confirming that an unmodified CT is required for AS-induced effects, and that fewer than six Cx26 monomers in a hemichannel are required for AS sensitivity (also shown in Locke et al., 2004b). AS causes pore narrowing of homomeric hemichannels in which the Cx26CT has the short addition (Cx26_{T_C}) but inhibits channel activity when the same Cx26 modification is in heteromeric (Cx26_{T_C}/Cx32) hemichannels. This suggests that there is some interaction between Cx26 and Cx32, which converts AS-induced pore narrowing into full closure, as if the Cx26CT was unmodified. One possibility is that at low pH, Cx26_{T_C} is able to recruit the Cx32CT to participate in pore occlusion. There is no obvious sequence similarity between the Cx32 and Cx26 CTs to suggest a basis for this, however, except that the initial segment of both have a preponderance of positively charged residues. An analogous possibility is that the CT of Cx26 recruits involvement of the CL of Cx32. These explanations would be most readily consistent with direct occlusion of the pore by free Cx26 CT or by free Cx26 CL+AS (mechanisms a and c above, respectively).

When the heteromeric channels contain Cx26 with the longer CT addition (Cx26_T/Cx32), there is no AS sensitivity at all. This is expected because homomeric Cx26_T channels are insensitive. The inability of Cx32 to reinstate the sensitivity to AS in this case suggests that the additional length of the CT in Cx26_T blocks the compensatory interaction with Cx32 that occurs in the Cx26_{T_C}/Cx32 channels. Moreover, the Cx32CT is significantly longer (69 amino acids; approximately six-fold) than the Cx26CT; in effect, the native Cx32CT mimics a Cx26CT with a large purification tag.

Relation to CL–CT interactions in other connexins

As noted above, the intramolecular basis of pH-driven gating in Cx43, an exemplar of the α connexin family, has been well described (Hirst-Jensen et al., 2007). Although it also involves interactions between the CT and the second half of the CL (a peptide called “L2”), there are strikingly different functional consequences. In Cx43, acidic conditions protonate histidine(s) in the L2, driving formation of an α helix that interacts with part of the CT, leading to occlusion of the channel pore.

The notion of dynamic interactions between CL and CT domains of connexins is supported by AFM studies indicating high structural flexibility of the cytoplasmic domains of Cx26, Cx40, and Cx43 (Müller et al., 2002; Liu et al., 2006; Allen et al., 2011), which could also be inferred from the inability to resolve these domains in the x-ray crystal structure (Maeda et al., 2009). AFM studies

have also shown changes in the conformations of the cytoplasmic domains of Cx40 and Cx43, with channel gating induced by Ca^{2+} (Liu et al., 2006; Allen et al., 2011).

At present, there is no structural information about pH-induced changes in secondary structure of the Cx26CL. Overall, there is little sequence similarity between the relevant segments (L2 of Cx43 and CL3 of Cx26). However, there is considerable similarity in a small segment of the first half of CL3 and the latter half of L2 (Fig. 6 A). It is tempting to think that this sequence and similarity of charge patterns play roles in structural responses to pH and interaction with the respective CTs.

A recent study examined the α -helical content of peptides corresponding to various connexin domains in the presence of trifluoroethanol, which tends to stabilize secondary structure (Fort and Spray, 2009). The propensity to form α helices thus revealed was substantial and equivalent for peptides corresponding to the L2 peptide of Cx43 and the CL3 peptide of Cx32. The overall similarity of the CL3 segments of Cx26 and Cx32 noted above suggests that the same propensity exists for Cx26 (Fig. 6 A), consistent with the transition in secondary structure of Cx43 that enables interaction with its CT.

Mutations and posttranslational modifications (PTMs) of the Cx26 CT and CL

Prior to this work, a functional or structural role for the Cx26CT in channel physiology was unknown. In other connexins, the CT is much longer and often contains sites for PTM (e.g., phosphorylation) as well as protein-protein interaction (e.g., SH2/PDZ-binding segments) (Sorgen et al., 2004; Solan and Lampe, 2009). As noted above, the CT of Cx26 has been considered too short to play an important functional role, be it involving PTMs or inter/intramolecular interactions.

However, several mutations that affect the Cx26CT cause nonsyndromic deafness (<http://davinci.crg.es/deafness/index.php>). A two-nucleotide deletion in codon 211 terminates the protein four codons later, eliminating the entire CT (Kelley et al., 1998). A four-base deletion starting in codon 215 causes a frameshift (Prasad et al., 2000). The CT deafness mutation L214P does not form functional channels (Meşe et al., 2004). Of interest, the deafness mutation K224Q (Antoniadi et al., 2000), which eliminates a basic, potential sulfonate-binding site on the Cx26CT, also does not form functional channels. Unfortunately, it is unknown whether the K224Q mutation interferes with channel biogenesis, trafficking, or plasma membrane insertion.

Channel function can also be modulated by PTMs. Mass spectrometry analysis indicated that either K221 or K223 in the Cx26CT could be methylated (Locke et al., 2009). This would not alter charge but would increase residue hydrophobicity and “bulk” of the CT. Several

PTMs of acidic residues (i.e., potential amine-binding sites) in the Cx26CL were also observed, as well as other modifications of the CL. None were detected in the CL3 portion (which had poor peptide ionization as a result of the hydrophobicity of this segment), but if residues in the CL3 portion of the CL are so modified, they could affect AS sensitivity.

Correlation with in vivo conditions

The studies of channel function reported here use hemichannels reconstituted into liposomes, and hemichannels and junctional channels expressed in cells. The molecular interactions that underlie this modulation of channel activity were explored using different biochemical techniques and several peptide reagents. Despite all of the differences in experimental strategies and conditions, the effects of AS and of the various CT alterations on AS sensitivity are highly correlated in all functional assays (activity and permeability studies of channels in liposomes and in native cells), channel forms (hemichannels and junctional channels), and molecular interaction studies (ELISA and NMR).

TSF, ELISA, and NMR conditions differ from those in cells. In addition, the behavior of the peptide segments will be affected by integration into the full connexin protein and by the quaternary structure of the channel in a membrane environment. Also, although no accessory proteins that affect Cx26 channel function have yet been identified, the possibility exists. Because of these factors, one should not presume that all inferences derived from studies of peptides will be directly applicable without modification to cellular physiology. However, we note that for many proteins, including Cx43, study of model peptides has been informative regarding function of intact channels in cells.

In the present study, taurine was used as the AS because of its ubiquitous yet inhomogeneous presence in biological tissues. Taurine is involved in a multitude of cellular processes, including anti-oxidation, modulation of cytosolic Ca^{2+} levels, and osmoregulation (Huxtable, 1992; Foos and Wu, 2002; Wu et al., 2005; Lambert et al., 2008; Schaffer et al., 2009; Pan et al., 2010). Its concentration in cells varies widely and is a function of the activities of several biosynthetic enzymes and taurine transporters, which are dynamically regulated (Huxtable, 1992; Lambert, 2004; Tappaz, 2004; Han et al., 2006). In this report, taurine is used as a tool, albeit with potential biological relevance, to explore molecular interactions involved in connexin channel gating.

To date, there are no hard data pointing to cytosolic taurine as a biologically used mechanism for modulation of connexin channel function, although it has been inferred (Locke et al., 2004b). However, we note that the action of taurine on Cx26-containing channels is shared by other cytoplasmic AS (e.g., L-cysteic acid, L-homocysteic acid, hypotaurine), some of which are

more effective than taurine (Tao and Harris, 2004). Where these compounds are enantiomeric, only the L-isomer is effective. Furthermore, several related cytoplasmic compounds that lack the sulfonate moiety (e.g., β -alanine, glycine, γ -aminobutyric acid) competitively antagonize the effect of taurine on these channels. Other cytoplasmic AS and related compounds not yet tested may also be effective. The presence of modulators and their competitive antagonists in cells allows for dynamic regulation of connexin channels.

The mechanism described here involves a pH-driven interdomain interaction that renders the Cx26-containing channels sensitive to AS. It would therefore come into play when there are changes in intracellular/local pH, such as are known to occur in glial cells during and after neuronal activity (Chesler and Kraig, 1989). In such a scenario, whether or not the cells remain coupled and thereby enable spatial buffering of extracellular K^+ and neurotransmitters would depend on the presence of, and interplay among, the cytosolic modulators of the CL-CT interaction.

Conclusions

These results have several broad implications for connexin channel structure–function. One is that the short CT of Cx26 is clearly involved in the intramolecular gating of connexin channels, in this case by an endogenous ligand, a unique finding. The fact that a four-amino acid extension of the Cx26CT narrows the pore with AS exposure suggests a direct role for the Cx26CT in modulation of the pore. This is the first demonstration of Cx26CT involvement in modulation of channel function.

We note the excellent correspondence between the AS physiologies observed with hemichannels in both cells and liposomes, and when docked to form gap junction channels between cells. Thus, the site(s) of AS action and associated gating mechanisms are retained in each system, and for this mechanism, at least, hemichannels are useful for study of the processes of AS-mediated channel closure.

Few ligands have been shown to directly and/or allosterically modulate connexin channels. By investigation of the connexin determinants of the actions of an endogenous modulatory ligand, these experimental findings inform the issues of both intersubunit and intrasubunit interactions, functional effects of the presence of more than one connexin isoform within a channel (i.e., heteromericity), sites of ligand modulation of connexin channels, and the structural segments capable of narrowing the pore. They have implications both for biological modulation of the channel and for the ability to manipulate the functionality of these channels, genetically and especially pharmacologically, to address outstanding biological and biophysical issues of intercellular signaling.

The authors wish to thank Jade Liu (University of Medicine and Dentistry of New Jersey [UMDNJ]) for technical assistance, Robert J. Donnelly (Molecular Research Core, UMDNJ) for peptides, and

Gina Sosinsky (University of California, San Diego) for HeLa cells expressing non-tagged Cx26.

This work was supported by National Institutes of Health grants GM072631 (to P.L. Sorgen), and GM36044 and GM61406 (to A.L. Harris).

Edward N. Pugh Jr. served as editor.

Submitted: 21 March 2011

Accepted: 18 July 2011

REFERENCES

- Allen, M.J., J. Gemel, E.C. Beyer, and R. Lal. 2011. Atomic force microscopy of connexin40 gap junction hemichannels reveals calcium-dependent three-dimensional molecular topography and open-closed conformations of both the extracellular and cytoplasmic faces. *J. Biol. Chem.* 286:22139–22146. doi:10.1074/jbc.M111.240002
- Antoniadi, T., K. Grønskov, A. Sand, A. Pampanos, K. Brøndum-Nielsen, and M.B. Petersen. 2000. Mutation analysis of the GJB2 (connexin 26) gene by DGGE in Greek patients with sensorineural deafness. *Hum. Mutat.* 16:7–12. doi:10.1002/1098-1004(200007)16:1<7::AID-HUMU2>3.0.CO;2-A
- Ayad, W.A., D. Locke, I.V. Koreen, and A.L. Harris. 2006. Heteromeric, but not homomeric, connexin channels are selectively permeable to inositol phosphates. *J. Biol. Chem.* 281:16727–16739. doi:10.1074/jbc.M600136200
- Bao, X., G.A. Altenberg, and L. Reuss. 2004. Mechanism of regulation of the gap junction protein connexin 43 by protein kinase C-mediated phosphorylation. *Am. J. Physiol. Cell Physiol.* 286:C647–C654. doi:10.1152/ajpcell.00295.2003
- Beahm, D.L., and J.E. Hall. 2002. Hemichannel and junctional properties of connexin 50. *Biophys. J.* 82:2016–2031. doi:10.1016/S0006-3495(02)75550-1
- Bevans, C.G., and A.L. Harris. 1999. Regulation of connexin channels by pH. Direct action of the protonated form of taurine and other aminosulfonates. *J. Biol. Chem.* 274:3711–3719. doi:10.1074/jbc.274.6.3711
- Bevans, C.G., M. Kordel, S.K. Rhee, and A.L. Harris. 1998. Isoform composition of connexin channels determines selectivity among second messengers and uncharged molecules. *J. Biol. Chem.* 273:2808–2816. doi:10.1074/jbc.273.5.2808
- Bukauskas, F.F., and V.K. Verselis. 2004. Gap junction channel gating. *Biochim. Biophys. Acta.* 1662:42–60. doi:10.1016/j.bbame.2004.01.008
- Chesler, M., and R.P. Kraig. 1989. Intracellular pH transients of mammalian astrocytes. *J. Neurosci.* 9:2011–2019.
- Contreras, J.E., J.C. Sáez, F.F. Bukauskas, and M.V.L. Bennett. 2003. Gating and regulation of connexin 43 (Cx43) hemichannels. *Proc. Natl. Acad. Sci. USA.* 100:11388–11393. doi:10.1073/pnas.1434298100
- D'Andrea, P., V. Veronesi, M. Bicego, S. Melchionda, L. Zelante, E. Di Iorio, R. Bruzzone, and P. Gasparini. 2002. Hearing loss: frequency and functional studies of the most common connexin26 alleles. *Biochem. Biophys. Res. Commun.* 296:685–691. doi:10.1016/S0006-291X(02)00891-4
- Foos, T.M., and J.Y. Wu. 2002. The role of taurine in the central nervous system and the modulation of intracellular calcium homeostasis. *Neurochem. Res.* 27:21–26. doi:10.1023/A:1014890219513
- Fort, A.G., and D.C. Spray. 2009. Trifluoroethanol reveals helical propensity at analogous positions in cytoplasmic domains of three connexins. *Biopolymers.* 92:173–182. doi:10.1002/bip.21166
- Goldberg, G.S., J.F. Bechberger, and C.C.G. Naus. 1995. A pre-loading method of evaluating gap junctional communication by fluorescent dye transfer. *Biotechniques.* 18:490–497.

- González-Nilo, F.D., H. Krautwurst, A. Yévenes, E. Cardemil, and R. Cachau. 2002. Saccharomyces cerevisiae phosphoenolpyruvate carboxykinase: theoretical and experimental study of the effect of glutamic acid 284 on the protonation state of lysine 213. *Biochim. Biophys. Acta*. 1599:65–71.
- Good, N.E., G.D. Winget, W. Winter, T.N. Connolly, S. Izawa, and R.M. Singh. 1966. Hydrogen ion buffers for biological research. *Biochemistry*. 5:467–477. doi:10.1021/bi00866a011
- Goodenough, D.A., and D.L. Paul. 2003. Beyond the gap: functions of unpaired connexon channels. *Nat. Rev. Mol. Cell Biol.* 4:285–294. doi:10.1038/nrm1072
- Green, G.E., D.A. Scott, J.M. McDonald, G.G. Woodworth, V.C. Sheffield, and R.J.H. Smith. 1999. Carrier rates in the midwestern United States for GJB2 mutations causing inherited deafness. *JAMA*. 281:2211–2216. doi:10.1001/jama.281.23.2211
- Halgren, T.A. 1996. Merck molecular force field. I. Basis, form, scope, parameterization, and performance of MMFF94. *J. Comput. Chem.* 17:490–519. doi:10.1002/(SICI)1096-987X(199604)17:5/6<490::AID-JCC1>3.0.CO;2-P
- Han, X., A.B. Patters, D.P. Jones, I. Zelikovic, and R.W. Chesney. 2006. The taurine transporter: mechanisms of regulation. *Acta Physiol. (Oxf.)*. 187:61–73. doi:10.1111/j.1748-1716.2006.01573.x
- Hand, G.M., D.J. Müller, B.J. Nicholson, A. Engel, and G.E. Sosinsky. 2002. Isolation and characterization of gap junctions from tissue culture cells. *J. Mol. Biol.* 315:587–600. doi:10.1006/jmbi.2001.5262
- Harris, A.L. 2001. Emerging issues of connexin channels: biophysics fills the gap. *Q. Rev. Biophys.* 34:325–472.
- Harris, A.L. 2007. Connexin channel permeability to cytoplasmic molecules. *Prog. Biophys. Mol. Biol.* 94:120–143. doi:10.1016/j.pbiomolbio.2007.03.011
- Harris, A.L., A. Walter, D.L. Paul, D.A. Goodenough, and J. Zimmerberg. 1992. Ion channels in single bilayers induced by rat connexin32. *Brain Res. Mol. Brain Res.* 15:269–280. doi:10.1016/0169-328X(92)90118-U
- Harris, T.K., and G.J. Turner. 2002. Structural basis of perturbed pKa values of catalytic groups in enzyme active sites. *IUBMB Life*. 53:85–98. doi:10.1080/15216540211468
- Heginbotham, L., L. Kolmakova-Partensky, and C. Miller. 1998. Functional reconstitution of a prokaryotic K⁺ channel. *J. Gen. Physiol.* 111:741–749.
- Hehre, W. 1973. A Guide to Molecular Mechanics and Quantum Chemical Calculations. Wavefunction, Inc., Irvine, CA. 812 pp.
- Hervé, J.C., and D. Sarrouilhe. 2005. Connexin-made channels as pharmacological targets. *Curr. Pharm. Des.* 11:1941–1958. doi:10.2174/1381612054021060
- Hirst-Jensen, B.J., P. Sahoo, F. Kieken, M. Delmar, and P.L. Sorgen. 2007. Characterization of the pH-dependent interaction between the gap junction protein connexin43 carboxyl terminus and cytoplasmic loop domains. *J. Biol. Chem.* 282:5801–5813. doi:10.1074/jbc.M605233200
- Homma, N., J.L. Alvarado, W. Coombs, K. Stergiopoulos, S.M. Taffet, A.F. Lau, and M. Delmar. 1998. A particle-receptor model for the insulin-induced closure of connexin43 channels. *Circ. Res.* 83:27–32.
- Huxtable, R.J. 1992. Physiological actions of taurine. *Physiol. Rev.* 72:101–163.
- Kelley, P.M., D.J. Harris, B.C. Comer, J.W. Askew, T. Fowler, S.D. Smith, and W.J. Kimberling. 1998. Novel mutations in the connexin 26 gene (GJB2) that cause autosomal recessive (DFNB1) hearing loss. *Am. J. Hum. Genet.* 62:792–799. doi:10.1086/301807
- Kim, D.Y., Y. Kam, S.K. Koo, and C.O. Joe. 1999. Gating connexin 43 channels reconstituted in lipid vesicles by mitogen-activated protein kinase phosphorylation. *J. Biol. Chem.* 274:5581–5587. doi:10.1074/jbc.274.9.5581
- Koreen, I.V., W.A. Elsayed, Y.J. Liu, and A.L. Harris. 2004. Tetracycline-regulated expression enables purification and functional analysis of recombinant connexin channels from mammalian cells. *Biochem. J.* 383:111–119. doi:10.1042/BJ20040806
- Lambert, I.H. 2004. Regulation of the cellular content of the organic osmolyte taurine in mammalian cells. *Neurochem. Res.* 29:27–63. doi:10.1023/B:NERE.0000010433.08577.96
- Lambert, I.H., E.K. Hoffmann, and S.F. Pedersen. 2008. Cell volume regulation: physiology and pathophysiology. *Acta Physiol. (Oxf.)*. 194:255–282. doi:10.1111/j.1748-1716.2008.01910.x
- Lampe, P.D., J. Kistler, A. Hefti, J. Bond, S. Müller, R.G. Johnson, and A. Engel. 1991. In vitro assembly of gap junctions. *J. Struct. Biol.* 107:281–290. doi:10.1016/1047-8477(91)90053-Y
- Lee, J.R., and T.W. White. 2009. Connexin-26 mutations in deafness and skin disease. *Expert Rev. Mol. Med.* 11:e35. doi:10.1017/S1462399409001276
- Li, H.Y., T.F. Liu, A. Lazrak, C. Peracchia, G.S. Goldberg, P.D. Lampe, and R.G. Johnson. 1996. Properties and regulation of gap junctional hemichannels in the plasma membranes of cultured cells. *J. Cell Biol.* 134:1019–1030. doi:10.1083/jcb.134.4.1019
- Liu, F., F.T. Arce, S. Ramachandran, and R. Lal. 2006. Nanomechanics of hemichannel conformations: connexin flexibility underlying channel opening and closing. *J. Biol. Chem.* 281:23207–23217. doi:10.1074/jbc.M605048200
- Locke, D., I.V. Koreen, J.Y. Liu, and A.L. Harris. 2004a. Reversible pore block of connexin channels by cyclodextrins. *J. Biol. Chem.* 279:22883–22892. doi:10.1074/jbc.M401980200
- Locke, D., T. Stein, C. Davies, J. Morris, A.L. Harris, W.H. Evans, P. Monaghan, and B. Gusterson. 2004b. Altered permeability and modulatory character of connexin channels during mammary gland development. *Exp. Cell Res.* 298:643–660. doi:10.1016/j.yexcr.2004.05.003
- Locke, D., J. Liu, and A.L. Harris. 2005. Lipid rafts prepared by different methods contain different connexin channels, but gap junctions are not lipid rafts. *Biochemistry*. 44:13027–13042. doi:10.1021/bi050495a
- Locke, D., S. Bian, H. Li, and A.L. Harris. 2009. Post-translational modifications of connexin26 revealed by mass spectrometry. *Biochem. J.* 424:385–398. doi:10.1042/BJ20091140
- Lurtz, M.M., and C.F. Louis. 2007. Intracellular calcium regulation of connexin43. *Am. J. Physiol. Cell Physiol.* 293:C1806–C1813. doi:10.1152/ajpcell.00630.2006
- Maeda, S., S. Nakagawa, M. Suga, E. Yamashita, A. Oshima, Y. Fujiyoshi, and T. Tsukihara. 2009. Structure of the connexin 26 gap junction channel at 3.5 Å resolution. *Nature*. 458:597–602. doi:10.1038/nature07869
- Mani, R.S., A. Ganapathy, R. Jalvi, C.R. Srikumari Srisailapathy, V. Malhotra, S. Chadha, A. Agarwal, A. Ramesh, R.R. Rangasayee, and A. Anand. 2009. Functional consequences of novel connexin 26 mutations associated with hereditary hearing loss. *Eur. J. Hum. Genet.* 17:502–509. doi:10.1038/ejhg.2008.179
- Meşe, G., E. Londin, R. Mui, P.R. Brink, and T.W. White. 2004. Altered gating properties of functional Cx26 mutants associated with recessive non-syndromic hearing loss. *Hum. Genet.* 115:191–199. doi:10.1007/s00439-004-1142-6
- Mukoyama, E.B., M. Oguchi, Y. Koder, T. Maeda, and H. Suzuki. 2004. Low pKa lysine residues at the active site of sarcosine oxidase from *Corynebacterium* sp. U-96. *Biochem. Biophys. Res. Commun.* 320:846–851. doi:10.1016/j.bbrc.2004.05.219
- Müller, D.J., G.M. Hand, A. Engel, and G.E. Sosinsky. 2002. Conformational changes in surface structures of isolated connexin 26 gap junctions. *EMBO J.* 21:3598–3607. doi:10.1093/emboj/cdf365
- Nicholson, B.J. 2003. Gap junctions—from cell to molecule. *J. Cell Sci.* 116:4479–4481. doi:10.1242/jcs.00821

- Palmada, M., K. Schmalisch, C. Böhmer, N. Schug, M. Pfister, F. Lang, and N. Blin. 2006. Loss of function mutations of the GJB2 gene detected in patients with DFNB1-associated hearing impairment. *Neurobiol. Dis.* 22:112–118. doi:10.1016/j.nbd.2005.10.005
- Pan, C., G.S. Giraldo, H. Prentice, and J.Y. Wu. 2010. Taurine protection of PC12 cells against endoplasmic reticulum stress induced by oxidative stress. *J. Biomed. Sci.* 17:S17. doi:10.1186/1423-0127-17-S1-S17
- Petegnief, V., P.L. Llew, R.C. Gupta, J.J. Bourguignon, and G. Rebel. 1995. Taurine analog modulation of taurine uptake by two different mechanisms in cultured glial cells. *Biochem. Pharmacol.* 49:399–410. doi:10.1016/0006-2952(94)00390-8
- Prasad, S., R.A. Cucci, G.E. Green, and R.J.H. Smith. 2000. Genetic testing for hereditary hearing loss: connexin 26 (GJB2) allele variants and two novel deafness-causing mutations (R32C and 645-648delTAGA). *Hum. Mutat.* 16:502–508. doi:10.1002/1098-1004(200012)16:6<502::AID-HUMU7>3.0.CO;2-4
- Quist, A.P., S.K. Rhee, H. Lin, and R. Lal. 2000. Physiological role of gap-junctional hemichannels. Extracellular calcium-dependent isotonic volume regulation. *J. Cell Biol.* 148:1063–1074. doi:10.1083/jcb.148.5.1063
- Ramamoorthy, S., F.H. Leibach, V.B. Mahesh, H. Han, T. Yang-Feng, R.D. Blakely, and V. Ganapathy. 1994. Functional characterization and chromosomal localization of a cloned taurine transporter from human placenta. *Biochem. J.* 300:893–900.
- Rhee, S.K., C.G. Bevans, and A.L. Harris. 1996. Channel-forming activity of immunoaffinity-purified connexin32 in single phospholipid membranes. *Biochemistry.* 35:9212–9223. doi:10.1021/bi960295m
- Sáez, J.C., M.A. Retamal, D. Basilio, F.F. Bukauskas, and M.V. Bennett. 2005. Connexin-based gap junction hemichannels: gating mechanisms. *Biochim. Biophys. Acta.* 1711:215–224. doi:10.1016/j.bbame.2005.01.014
- Schaffer, S.W., J. Azuma, and M. Mozaffari. 2009. Role of antioxidant activity of taurine in diabetes. *Can. J. Physiol. Pharmacol.* 87:91–99. doi:10.1139/Y08-110
- Schalper, K.A., J.A. Orellana, V.M. Berthoud, and J.C. Sáez. 2009. Dysfunctions of the diffusional membrane pathways mediated by hemichannels in inherited and acquired human diseases. *Curr. Vasc. Pharmacol.* 7:486–505. doi:10.2174/157016109789043937
- Schulte, U., H. Hahn, M. Konrad, N. Jeck, C. Derst, K. Wild, S. Weidemann, J.P. Ruppersberg, B. Fakler, and J. Ludwig. 1999. pH gating of ROMK (K(ir)1.1) channels: control by an Arg-Lys-Arg triad disrupted in antenatal Bartter syndrome. *Proc. Natl. Acad. Sci. USA.* 96:15298–15303. doi:10.1073/pnas.96.26.15298
- Seifert, R., E. Eismann, J. Ludwig, A. Baumann, and U.B. Kaupp. 1999. Molecular determinants of a Ca²⁺-binding site in the pore of cyclic nucleotide-gated channels: S5/S6 segments control affinity of intrapore glutamates. *EMBO J.* 18:119–130. doi:10.1093/emboj/18.1.119
- Solan, J.L., and P.D. Lampe. 2009. Connexin43 phosphorylation: structural changes and biological effects. *Biochem. J.* 419:261–272. doi:10.1042/BJ20082319
- Sorgen, P.L., H.S. Duffy, P. Sahoo, W. Coombs, M. Delmar, and D.C. Spray. 2004. Structural changes in the carboxyl terminus of the gap junction protein connexin43 indicates signaling between binding domains for c-Src and zonula occludens-1. *J. Biol. Chem.* 279:54695–54701. doi:10.1074/jbc.M409552200
- Sosinsky, G.E., and B.J. Nicholson. 2005. Structural organization of gap junction channels. *Biochim. Biophys. Acta.* 1711:99–125.
- Spray, D.C., Z.C. Ye, and B.R. Ransom. 2006. Functional connexin “hemichannels”: a critical appraisal. *Glia.* 54:758–773. doi:10.1002/glia.20429
- Srinivas, M., J. Kronengold, F.F. Bukauskas, T.A. Bargiello, and V.K. Verselis. 2005. Correlative studies of gating in Cx46 and Cx50 hemichannels and gap junction channels. *Biophys. J.* 88:1725–1739. doi:10.1529/biophysj.104.054023
- Srinivas, M., D.P. Calderon, J. Kronengold, and V.K. Verselis. 2006. Regulation of connexin hemichannels by monovalent cations. *J. Gen. Physiol.* 127:67–75. doi:10.1085/jgp.200509397
- Stergiopoulos, K., J.L. Alvarado, M. Mastroianni, J.F. Ek-Vitorin, S.M. Taffet, and M. Delmar. 1999. Hetero-domain interactions as a mechanism for the regulation of connexin channels. *Circ. Res.* 84:1144–1155.
- Tao, L., and A.L. Harris. 2004. Biochemical requirements for inhibition of connexin26-containing channels by natural and synthetic taurine analogs. *J. Biol. Chem.* 279:38544–38554. doi:10.1074/jbc.M405654200
- Tao, L., and A.L. Harris. 2007. 2-aminoethoxydiphenyl borate directly inhibits channels composed of connexin26 and/or connexin32. *Mol. Pharmacol.* 71:570–579. doi:10.1124/mol.106.027508
- Tappaz, M.L. 2004. Taurine biosynthetic enzymes and taurine transporter: molecular identification and regulations. *Neurochem. Res.* 29:83–96. doi:10.1023/B:NERE.0000010436.44223.f8
- Weber, P.A., H.C. Chang, K.E. Spaeth, J.M. Nitsche, and B.J. Nicholson. 2004. The permeability of gap junction channels to probes of different size is dependent on connexin composition and permeant-pore affinities. *Biophys. J.* 87:958–973. doi:10.1529/biophysj.103.036350
- Willecke, K., J. Eiberger, J. Degen, D. Eckardt, A. Romualdi, M. Güldenagel, U. Deutsch, and G. Söhl. 2002. Structural and functional diversity of connexin genes in the mouse and human genome. *Biol. Chem.* 383:725–737. doi:10.1515/BC.2002.076
- Wu, H., Y. Jin, J. Wei, H. Jin, D. Sha, and J.Y. Wu. 2005. Mode of action of taurine as a neuroprotector. *Brain Res.* 1038:123–131. doi:10.1016/j.brainres.2005.01.058
- Yu, J., C.A. Bippes, G.M. Hand, D.J. Müller, and G.E. Sosinsky. 2007. Aminosulfonate modulated pH-induced conformational changes in connexin26 hemichannels. *J. Biol. Chem.* 282:8895–8904. doi:10.1074/jbc.M609317200
- Zhang, J.T., and B.J. Nicholson. 1989. Sequence and tissue distribution of a second protein of hepatic gap junctions, Cx26, as deduced from its cDNA. *J. Cell Biol.* 109:3391–3401. doi:10.1083/jcb.109.6.3391
- Zoidl, G., and R. Dermietzel. 2010. Gap junctions in inherited human disease. *Pflugers Arch.* 460:451–466. doi:10.1007/s00424-010-0789-1